localization of p53 might be involved in the genesis and development of HBL, and the acetylation status of p53 plays an important role in the cytoplasmic retention of p53. Furthermore, the oxidative stress-induced apoptotic cell death in Huh6 cells was strongly associated with the active nuclear translocation of p53, which was distinct from the CDDP-mediated nuclear accumulation of p53. Thus, our present results provide a novel targeted approach to enhance the HBL cell cytotoxity.

Experimental procedures

Cell culture

Human hepatoblastoma Huh6 cells and human hepatocellular carcinoma HepG2 cells were cultured in Dulbecco's modified Eagle's medium (DMEM) supplemented with 10% heat-inactivated fetal bovine serum (FBS; Invitrogen, Carlsbad, CA) and penicillin (100 IU/mL)/streptomycin (100 μg/mL). Cultures were maintained at 37 °C in a water-saturated atmosphere of 5% CO_2 in air.

RNA preparation and RT-PCR

Total RNA was extracted from cells exposed to cisplatin or hydrogen peroxide using the RNeasy Mini kit (Qiagen, Valencia, CA) according to the manufacturer's protocol. cDNA was reverse transcribed from 1 μg of total RNA with random primers and SuperScript II (Invitrogen) as recommended by the supplier. Following the reverse transcription, the resultant cDNA was subjected to the PCR-based amplification. For PCR analysis, oligonucleotide sequences used were as follows: *NOXA*, 5′-GCAAGAATGGAAGACCCTTG-3′ and 5′-GTGCTGAGTTGGCACTGAAA-3′; *Parc*, 5′-CGTCTCCTGAGCTTTGGTTC-3′ and 5′-CCTCATCTTCCTGCTCCAAG-3′; *GAPDH*, 5′-ACCTGACCTGCCGTCTAGAA-3′ and 5′-TCCACCACCCTGTTGCTGTA-3′. PCR products were resolved by 2% agarose gel electrophoresis, and visualized by ethidium bromide staining.

Western blot analysis

Cells were rinsed twice in ice-cold PBS and lyzed in SDS sample buffer containing 62.5 mM Tris–HCl, pH 6.8, 2% SDS, 2% β-mercaptoethanol and 0.01% bromophenol blue, followed by a brief sonication. After centrifugation at 10 000 *g* for 10 min at 4 °C, the supernatant was transferred to a new tube. The protein concentration was measured by the Bradford protein assay (Bio-Rad laboratories, Hercules, CA), using bovine serum albumin as a standard. For Western analysis, equal amounts of protein were separated by 10% SDS-PAGE, and electro-transferred on to Immobilon-P membranes (Millipore, Bedford, MA). The membranes were blocked overnight at 4 °C with TBS-T (50 mM Tris–HCl, pH 8.0, 100 mM NaCl and 0.1% Tween 20) containing 5% non-fat dry milk, and then incubated for 1 h at room temperature with the monoclonal anti-p53 (DO-1; Oncogene Research Products, Cambridge, MA), polyclonal anti-phosphorylated p53 at Ser-15 (Cell Signaling Technology, Beverly, MA), polyclonal anti-Parc (Calbiochem, La Jolla), or with polyclonal anti-actin antibody (20–33; Sigma Chemical Co., St. Louis, MO). After washing with TBS-T, the membranes were incubated with a horseradish peroxidase-conjugated appropriate secondary antibody (Jackson ImmunoResearch Laboratories, West Grove, PA) for 1 h at room temperature. The chemiluminescence reaction was performed using the ECL reagent (Amersham Biosciences, Piscataway, NJ).

Subcellular fractionation

Cells were washed twice in ice-cold PBS and lyzed in lysis buffer (10 mM Tris–HCl, pH 7.5, 1 mM EDTA, 0.5% NP-40) containing a protease inhibitor mix (Sigma Chemical Co.) for 10 min at 4 °C. Cell lysates were centrifuged at 10 000 *g* for 10 min at 4 °C to separate cytoplasmic fraction (supernatant). Insoluble materials were washed three times with the lysis buffer and nuclei were lyzed in 1× SDS sample buffer. The nuclear lysates were sonicated, centrifuged, and the supernatant was collected. The protein concentrations were determined by the Bradford protein assay (Bio-Rad Laboratories). The nuclear and cytoplasmic fractions were subjected to immunoblot analysis using the monoclonal anti-Lamin B (Ab-1; Oncogene Research Products) or monoclonal anti-α-tubulin antibody (Ab-2; NeoMarkers, Inc., Fremont, CA).

Indirect immunofluorescence

Huh6 cells on cover slips were fixed in ice-cold methanol for 5 min at room temperature and permeabilized with 0.2% Triton X-100 for 3 min at room temperature. After blocking with 3% bovine serum albumin in PBS, cover slips were incubated with anti-p53 antibody (DO-1) in PBS for 1 h at room temperature followed by incubation with rhodamine-conjugated secondary antibody (Invitrogen) in PBS for 1 h at room temperature. Cell nuclei were stained with DAPI.

Co-immunoprecipitation experiments

For co-immunoprecipitation experiments, cells were lyzed in lysis buffer (25 mM Tris–HCl, pH 8.0, 137 mM NaCl, 2.7 mM KCl, 1% Triton X-100) supplemented with protease inhibitor mixture for 30 min at 4 °C, and clarified by centrifugation at 10 000 *g* for 15 min at 4 °C. Equal amounts of whole cell lysates were precleared by incubation with 30 μL of 50% slurry of protein G-Sepharose beads (Amersham Biosciences). After brief centrifugation, the supernatants were collected and incubated with the normal mouse serum (NMS), or with monoclonal anti-p53 antibody (DO-1; Oncogene Research Products) at 4 °C for 2 h. The immune complexes were precipitated with the protein G-Sepharose beads for 1 h at 4 °C, and the nonspecific bound proteins were removed by washing the beads with the lysis buffer three times at 4 °C. Immunoprecipitated proteins were subjected to 10% SDS-PAGE, and Western blot analysis was carried out using the polyclonal anti-Parc antibody.

siRNA-mediated knockdown of p53

Huh6 cells were transfected with 2 μg of the empty plasmid (pSUPER; OligoEngine, Seattle, WA) or with pSUPER expression plasmid encoding siRNA against p53 (pSUPER-siRNA-p53) by using FuGENE 6 transfection reagent as recommended by the manufacturer (Roche Molecular Biochemicals, Mannheim, Germany). Forty-eight hours after transfection, the transfected cells were put under a selection pressure of 400 μg/mL of G418 (Sigma Chemical Co.). Thereafter, the selection medium was replaced every 3 days. Two weeks after the selection in G418, drug-resistant clones were isolated and allow to proliferate in medium containing G418 (400 μg/mL).

Cell survival assay

Cell viability was determined by MTT assay and expressed as percent viable cells. In brief, Huh6 or HepG2 cells were seeded in 96-well microtiter plates (5×10^3 cells/well) with 100 μL of complete medium. The next day, the medium was changed and cells were exposed to the indicated concentrations of hydrogen peroxide. At the indicated time periods after the treatment with hydrogen peroxide, 10 μL of MTT labeling reagent were added to each well, and the cultures were incubated for 1 h at 37 °C. The absorbance readings for each well were carried out at a wavelength of 570 nm using the microplate reader (model 450; Bio-Rad Laboratories).

Apoptotic analysis

Apoptotic cells were detected by *In Site* Cell Death Detection Kit, TMR red (Roche Molecular Biochemicals). In brief, Huh6 cells were grown overnight on glass cover slips at 37 °C. Five hours after the treatment with hydrogen peroxide, cells were washed in PBS, fixed in 4% paraformaldehyde for 1 h at room temperature and then permeabilized with 0.1% Triton X-100 for 2 min on ice. The cells were subsequently incubated with TUNEL reaction mixture for 1 h at 37 °C in a humidified atmosphere in the dark. The cover slips were mounted onto microscope slides using the VECTASHIELD containing DAPI (Vector Laboratories, Burlingame, CA), and examined under a Fluoview laser scanning confocal microscope (Olympus, Tokyo, Japan).

Tumor tissues and immunohistochemistry

Hepatoblastoma tissues, which were collected at Gunma Children's Medical Center, were obtained at surgery, immediately frozen and stored at −80 °C until use. Sections from formalin-fixed, paraffin-embedded tumor samples were cut at 4-μm thickness and subjected to immunostaining. In brief, antigen retrieval was achieved by the treatment of deparaffinized sections with microwaves in 0.1 M citrate buffer (pH 6.0) for 20 min, followed by cooling at room temperature prior to incubation with the primary antibody. Tissue sections were incubated with monoclonal anti-p53 antibody (PAb240; Calbiochem) overnight at 4 °C and washed in PBS. The bound antibody was detected using the strepto-avidin-biotin complex method (Nichirei Corp., Tokyo, Japan) and visualized by diaminobenzidine tetrahydrochloride.

Acknowledgements

We are grateful to Dr M. Kuroiwa for kindly providing the hepatoblastoma tissues and Ms Y. Nakamura for assistance with DNA sequencing. This work was supported in part by a Grant-in-Aid from the Ministry of Health, Labour and Welfare for Third Term Comprehensive Control Research for Cancer, a Grant-in-Aid for Scientific Research on Priority Areas from the Ministry of Education, Culture, Sports, Science and Technology of Japan, a Grant-in-Aid for Scientific Research from Japan Society for the Promotion of Science, and a Grant from Uehara Memorial Foundation.

References

Aberle, H., Bauer, A., Stappert, J., Kispert, A. & Kemler, R. (1997) β-catenin is a target for the ubiquitin-proteasome pathway. *EMBO J.* **16**, 3797–3804.

Aden, D.P., Fogel, A., Plotkin, S., Damjanov, I. & Knowles, B.B. (1979) Controlled synthesis of HBsAg in a differentiated human liver carcinoma-derived cell line. *Nature* **282**, 615–616.

Bosari, S., Viale, G., Roncalli, M., Graziani, D., Borsani, G., Lee, A.K. & Coggi, G. (1995) p53 gene mutations, p53 protein accumulation and compartmentalization in colorectal adenocarcinoma. *Am. J. Pathol.* **147**, 790–798.

Bressac, B., Galvin, K.M., Liang, J., Isselbacher, K.J., Wands, J.R. & Ozturk, M. (1990) Abnormal structure and expression of p53 gene in human hepatocellular carcinoma. *Proc. Natl. Acad. Sci. USA* **87**, 1973–1977.

Brooks, C.L. & Gu, W. (2003) Ubiquitination, phosphorylation and acetylation: the molecular basis for p53 regulation. *Curr. Opin. Cell Biol.* **15**, 164–171.

Chen, T.C., Hsieh, L.L. & Kuo, T.T. (1995) Absence of p53 gene mutation and infrequent overexpression of p53 protein in hepatoblastoma. *J. Pathol.* **176**, 243–247.

Chen, J., Marechal, V. & Levine, A.J. (1993) Mapping of the p53 and mdm-2 interaction domains. *Mol. Cell. Biol.* **13**, 4107–4114.

Doi, I. (1976) Establishment of a cell line and its clonal sublines from a patient with hepatoblastoma. *Gann* **67**, 1–10.

Dornan, D., Wertz, I., Shimizu, H., Arnott, D., Frantz, G.D., Dowd, P., O'Rourke, K., Koeppen, H. & Dixit, V.M. (2004) The ubiquitin ligase COP1 is a critical negative regulator of p53. *Nature* **429**, 86–92.

Fritsche, M., Haessler, C. & Brandner, G. (1993) Induction of nuclear accumulation of the tumor-suppressor protein p53 by DNA-damaging agents. *Oncogene* **8**, 307–318.

Gu, W. & Roeder, R.G. (1997) Activation of p53 sequence-specific DNA binding by acetylation of the p53 C-terminal domain. *Cell* **90**, 595–606.

Harada, N., Miyoshi, H., Murai, N., Oshima, H., Tamai, Y., Oshima, M. & Taketo, M.M. (2002) Lack of tumorigenesis in the mouse liver after adenovirus-mediated expression of a dominant stable mutant of β-catenin. *Cancer Res.* **62**, 1971–1977.

Harada, N., Oshima, H., Katoh, M., Tamai, Y., Oshima, M. & Taketo, M.M. (2004) Hepatocarcinogenesis in mice with β-catenin and Ha-ras gene mutations. *Cancer Res.* **64**, 48–54.

Haupt, Y., Maya, R., Kazaz, A. & Oren, M. (1997) Mdm2 promotes the rapid degradation of p53. *Nature* **387**, 296–299.

Henderson, B.R. & Fagotto, F. (2002) The ins and outs of APC and β-catenin nuclear transport. *EMBO Rep.* **3**, 834–839.

Hollstein, M., Sidransky, D., Vogelstein, B. & Harris, C.C. (1991) p53 mutations in human cancers. *Science* **253**, 49–53.

Honda, R., Tanaka, H. & Yasuda, H. (1997) Oncoprotein MDM2 is a ubiquitin ligase E3 for tumor suppressor p53. *FEBS Lett.* **420**, 25–27.

Hsu, I.C., Tokiwa, T., Bennett, W., Metcalf, R.A., Welsh, J.A., Sun, T. & Harris, C.C. (1993) p53 gene mutation and integrated hepatitis B viral DNA sequences in human liver cancer cell lines. *Carcinogenesis* **14**, 987–992.

Hughes, L.J. & Michels, V.V. (1992) Risk of hepatoblastoma in familial adenomatous polyposis. *Am. J. Med. Genet.* **43**, 1023–1025.

Kawaguchi, Y., Ito, A., Appella, E. & Yao, T.P. (2006) Charge modification at multiple C-terminal lysine residues regulates p53 oligomerization and its nucleus-cytoplasm trafficking. *J. Biol. Chem.* **281**, 1394–1400.

Koch, A., Denkhaus, D., Albrecht, S., Leuschner, I., von Schweinitz, D. & Pietsch, T. (1999) Childhood hepatoblastomas frequently carry a mutated degradation targeting box of the β-catenin gene. *Cancer Res.* **59**, 269–273.

Kubbutat, M.H., Jones, S.N. & Vousden, K.H. (1997) Regulation of p53 stability by Mdm2. *Nature* **387**, 299–303.

Kusafuka, T., Fukuzawa, M., Oue, T., Komoto, Y., Yoneda, A. & Okada, A. (1997) Mutation analysis of p53 gene in childhood malignant solid tumors. *J. Pediatr. Surg.* **32**, 1175–1180.

Leng, R.P., Lin, Y., Ma, W., Wu, H., Lemmers, B., Chung, S., Parant, J.M., Lozano, G., Hakem, R. & Benchimol, S. (2003) Pirh2, a p53-induced ubiquitin-protein ligase, promotes p53 degradation. *Cell* **112**, 779–791.

Llovet, J.M., Burroughs, A. & Bruix, J. (2003) Hepatocellular carcinoma. *Lancet* **362**, 1907–1917.

Lluis, J.M., Morales, A., Biasco, C., Colell, A., Mari, M., Garcia-Ruiz, C. & Fernandez-Checa, J.C. (2005) Critical role of mitochondrial glutathione in the survival of hepatocytes during hypoxia. *J. Biol. Chem.* **280**, 3224–3232.

Michishita, E., Park, J.Y., Burneskis, J.M., Barrett, J.C. & Horikawa, I. (2005) Evolutionarily conserved and nonconserved cellular localizations and functions of human SIRT proteins. *Mol. Biol. Cell* **16**, 4623–4635.

Moll, U.M., LaQuaglia, M., Benard, J. & Riou, G. (1995) Wild-type p53 protein undergoes cytoplasmic sequestration in undifferentiated neuroblastomas but not in differentiated tumors. *Proc. Natl. Acad. Sci. USA* **92**, 4407–4411.

Moll, U.M., Riou, G. & Levine, A.J. (1992) Two distinct mechanisms alter p53 in breast cancer: mutation and nuclear exclusion. *Proc. Natl. Acad. Sci. USA* **89**, 7262–7266.

Nagase, H. & Nakamura, Y. (1993) Mutations of the APC (adenomatous polyposis coli) gene. *Hum. Mutat.* **2**, 425–434.

Nikolaev, A.Y., Li, M., Puskas, N., Qin, J. & Gu, W. (2003) Parc: a cytoplasmic anchor for p53. *Cell* **112**, 29–40.

North, B.J., Marshall, B.L., Borra, M.T., Denu, J.M. & Verdin, E. (2003) The human Sir2 ortholog, SIRT2, is an NAD^+-dependent tubulin deacetylase. *Mol. Cell* **11**, 437–444.

Ogryzko, V.V., Schiltz, R.L., Russanova, V., Howard, B.H. & Nakatani, Y. (1996) The transcriptional coactivators p300 and CBP are histone acetyltransferases. *Cell* **29**, 953–959.

Ohnishi, H., Kawamura, M., Hanada, R., Kaneko, Y., Tsunoda, Y., Hongo, T., Bessho, F., Yokomori, K. & Hayashi, Y. (1996) Infrequent mutations of the TP53 gene and no amplification of the MDM2 gene in hepatoblastomas. *Genes Chromosomes Cancer* **15**, 187–190.

Ostermeyer, A.G., Runko, E., Winkfield, B., Ahn, B. & Moll, U.M. (1996) Cytoplasmically sequestered wild-type p53 protein in neuroblastoma is relocated to the nucleus by a C-terminal peptide. *Proc. Natl. Acad. Sci. USA* **93**, 15190–15194.

Prives, C. & Hall, P.A. (1999) The p53 pathway. *J. Pathol.* **187**, 112–126.

de Ruijter, A.J., van Gennip, A.H., Caron, H.N., Kemp, S. & van Kuilenburg, A.B. (2003) Histone deacetylases (HDACs): characterization of the classical HDAC family. *Biochem. J.* **370**, 737–749.

Shieh, S.Y., Ikeda, M., Taya, Y. & Prives, C. (1997) DNA damage-induced phosphorylation of p53 alleviates inhibition by MDM2. *Cell* **91**, 325–334.

Sionov, R.V. & Haupt, Y. (1999) The cellular response to p53: the decision between life and death. *Oncogene* **18**, 6145–6157.

Stommel, J.M., Marchenko, N.D., Jimenez, G.S., Moll, U.M., Hope, T.J. & Wahl, G.M. (1999) A leucine-rich nuclear export signal in the p53 tetramerization domain: regulation of subcellular localization and p53 activity by NES masking. *EMBO J.* **18**, 1660–1672.

Takayasu, H., Horie, H., Hiyama, E., Matsunaga, T., Hayashi, Y., Watanabe, Y., Suita, S., Kaneko, M., Sasaki, F., Hashizume, K., Ozaki, T., Furuuchi, K., Tada, M., Ohnuma, N. & Nakagawara, A. (2001) Frequent deletions and mutations of the β-catenin gene are associated with overexpression of cyclin D1 and fibronectin and poorly differentiated histology in childhood hepatoblastoma. *Clin. Cancer Res.* **7**, 901–908.

Vogan, K., Berstein, M., Leclerc, J.M., Brisson, L., Brossard, J., Brodeur, G.M., Pelletier, J. & Gros, P. (1993) Absence of p53 gene mutations in primary neuroblastomas. *Cancer Res.* **53**, 5269–5273.

Vogelstein, B., Lane, D. & Levine, A.J. (2000) Surfing the p53 network. *Nature* **408**, 307–310.

Vousden, K.H. & Lu, X. (2002) Live or let die: the cell's response to p53. *Nat. Rev. Cancer* **2**, 594–604.

Watcharasit, P., Bijur, G.N., Song, L., Zhu, J., Chen, X. & Jope, R.S. (2003) Glycogen synthase kinase-3β (GSK3β) binds to and promotes the actions of p53. *J. Biol. Chem.* **278**, 48872–48879.

Watcharasit, P., Bijur, G.N., Zmijewski, J.W., Song, L., Zmijewska, A., Chen, X., Johnson, G.V. & Jope, R.S. (2002) Direct, activating interaction between glycogen synthase kinase-3β and p53 after DNA damage. *Proc. Natl. Acad. Sci. USA* **99**, 7951–7955.

Received: 20 October 2006
Accepted: 21 December 2006

Available online at www.sciencedirect.com
ScienceDirect
ELSEVIER
Biochemical and Biophysical Research Communications 354 (2007) 892–898
BBRC
www.elsevier.com/locate/ybbrc

Functional characterization of a new p53 mutant generated by homozygous deletion in a neuroblastoma cell line

Yohko Nakamura [1], Toshinori Ozaki [1], Hidetaka Niizuma, Miki Ohira, Takehiko Kamijo, Akira Nakagawara *

Division of Biochemistry, Chiba Cancer Center Research Institute, Chiba 260-8717, Japan

Received 11 January 2007
Available online 22 January 2007

Abstract

p53 is a key modulator of a variety of cellular stresses. In human neuroblastomas, p53 is rarely mutated and aberrantly expressed in cytoplasm. In this study, we have identified a novel p53 mutant lacking its COOH-terminal region in neuroblastoma SK-N-AS cells. p53 accumulated in response to cisplatin (CDDP) and thereby promoting apoptosis in neuroblastoma SH-SY5Y cells bearing wild-type *p53*, whereas SK-N-AS cells did not undergo apoptosis. We found another p53 (p53ΔC) lacking a part of oligomerization domain and nuclear localization signals in SK-N-AS cells. p53ΔC was expressed largely in cytoplasm and lost the transactivation function. Furthermore, a 3′-part of the *p53* locus was homozygously deleted in SK-N-AS cells. Thus, our present findings suggest that p53 plays an important role in the DNA-damage response in certain neuroblastoma cells and it seems to be important to search for *p53* mutations outside DNA-binding domain.

Keywords: Apoptosis; Cisplatin; Homozygous deletion; Neuroblastoma; p53

p53 plays a pivotal role in the regulation of cell cycle arrest and apoptosis. *p53* is one of the most frequently mutated genes in human tumors [1,2] and *p53*-deficient mice developed spontaneous tumors [3]. Upon a variety of cellular stresses, p53 accumulates in nucleus through post-translational modifications including phosphorylation and acetylation and thereby exerting its function [4]. Pro-apoptotic function of p53 is closely linked to its DNA-binding activity. p53 acts as a transcription factor to transactivate a variety of its target genes. Indeed, 95% of *p53* mutations in human tumors occur within its DNA-binding region and these mutations inactivate pro-apoptotic function of p53 [4].

Alternatively, p53 is inhibited by various mechanisms. MDM2 acts as an E3 ubiquitin ligase for p53 and promotes its proteolytic degradation through ubiquitin–proteasome pathway [5,6]. Subcellular distribution of p53 also plays a key role in the regulation of p53 [4]. p53 contains three nuclear localization signals (NLS I, II, and III) in its COOH-terminal region [7,8]. In contrast to other human tumors, *p53* is rarely mutated in neuroblastomas [9]. Neuroblastoma cells showed a cytoplasmic localization of wild-type p53 and exhibited an impaired p53-mediated cell cycle arrest in response to DNA damage, suggesting that there exists a mutation-independent mechanism of p53 inactivation [10–12]. Intriguingly, Nikolaev et al. demonstrated that Parkin-like ubiquitin ligase termed Parc serves as an anchor protein that tethers p53 in cytoplasm and thereby regulating subcellular localization and function of p53 [13].

In this study, we have identified a novel p53 mutant (p53ΔC) homozygously deleted in neuroblastoma SK-N-AS cells and our current studies suggest that *p53* status plays an important role in the cell fate determination of certain neuroblastoma cells in response to DNA damage.

* Corresponding author. Fax: +81 43 265 4459.
E-mail address: akiranak@chiba-cc.jp (A. Nakagawara).
[1] These authors contributed equally to this work.

0006-291X/$ - see front matter © 2007 Elsevier Inc. All rights reserved.
doi:10.1016/j.bbrc.2007.01.057

Materials and methods

Cell culture and transfection. Neuroblastoma cells were grown in RPMI 1640 medium supplemented with 10% heat-inactivated fetal bovine serum (FBS, Invitrogen) and antibiotic mixture in a humidified atmosphere of 5% CO_2 in air at 37 °C. For transfection, cells were transfected with the indicated expression plasmids using LipofectAMINE 2000 according to the manufacturer's instructions (Invitrogen).

Construction of p53 mutant. cDNA encoding p53 mutant was amplified by PCR using cDNA from SK-N-AS cells. Forward and reverse primers were 5′-AATATTTCACCCTTCAGGTACTAAG-3′ (forward) and 5′-CTCGAGTCACTGCCCCCTGATGGC-3′ (reverse). *Ssp*I and *Xho*I sites shown in boldface type were introduced into forward and reverse primers, respectively. PCR products were gel-purified and subcloned into pGEM-T plasmid (Promega). Constructs were confirmed by sequencing and then digested with *Ssp*I and *Xho*I. The digested fragment was again gel-purified and then ligated with the *Ssp*I and *Bam*HI fragment of FLAG-p53 to give pcDNA3-FLAG-p53CΔ.

RNA preparation and RT-PCR analysis. Total RNA was prepared using RNeasy Mini kit (Qiagen) following the manufacturer's protocol. cDNA was synthesized using SuperScript II with random primers (Invitrogen) and amplified by PCR using primers as described: *p53*: forward, 5′-CTGCCCTCAACAAGATGTTTTG-3′, and reverse, 5′-CTATCTGAGCAGCGCTCATGG-3′; *p21^{WAF1}*: forward, 5′-ATGAAATTCACCCCCTTTCC-3′, and reverse, 5′-CCCTAGGCTGTGCTCACTTC-3′; *Bax*: forward, 5′-TTTGCTTCAGGGTTTCATCC-3′, and reverse, 5′-CAGTTGAAGTTGCCGTCAGA-3′; *p53AIP1*: forward, 5′-CCAAGTTCTCTGCTTTC-3′ and reverse, 5′-AGCTGAGCTCAAATGCTGAC-3′; *PUMA*: forward, 5′-TATGGATCCCGCACCATGGACTACAAGGACGACGATGACAAGGCCCGCGCACGCCAG-3′ and reverse, 5′-TATGGATCCCTACATGGTGCAGAGAAAGTCCCCC-3′; and *GAPDH*: forward, 5′-ACCTGACCTGCCGTCTAGAA-3′, and reverse, 5′-TCCACCACCCTGTTGCTGTA-3′.

Southern blotting. Genomic DNA was digested with *Pst*I, separated by 1% agarose gel electrophoresis, and transferred onto nylon membranes. Hybridization was performed at 65 °C in a solution containing 1 M NaCl, 1% *N*-lauroyl sarcosine, 7.5% dextran sulfate, 100 μg of heat-denatured salmon sperm DNA/ml, and radio-labeled DNA. After hybridization, membranes were washed twice with 2× SSC/0.1% *N*-lauroyl sarcosine at 50 °C and exposed to an X-ray film at −70 °C.

Immunoblotting. Cells were lysed in lysis buffer containing 25 mM Tris–HCl, pH 8.0, 137 mM NaCl, 2.7 mM KCl, 1% Triton X-100, and protease inhibitor mixture (Sigma). Lysates were separated by SDS–PAGE and transferred onto Immobilon-P membranes (Millipore). Membranes were probed with anti-p53 (DO-1, Calbiochem), anti-p53 (PAb122, BD Pharmingen), anti-phosphorylated p53 at Ser-15 (Cell Signaling) or with anti-actin (20–33, Sigma) followed by incubation with HRP-conjugated goat anti-mouse or anti-rabbit IgG secondary antibody (Cell Signaling). Immunoreactive bands were detected using chemiluminescence (ECL, Amersham Biosciences).

Subcellular fractionation. Cells were lysed in lysis buffer containing 10 mM Tris–HCl, pH 7.5, 1 mM EDTA, 0.5% NP-40, and protease inhibitor mixture (Sigma). Lysates were centrifuged to separate soluble (cytosolic) from insoluble (nuclear) fractions. The nuclear and cytosolic fractions were subjected to immunoblotting using anti-p53, anti-Lamin B (Ab-1, Oncogene Research products) or with anti-tubulin-α (Ab-2, NeoMarkers).

Array-based comparative genomic hybridization (CGH) analysis. Whole genome arrays of 2464 bacterial artificial chromosome (BAC) clones were hybridized simultaneously with 500 ng of target DNA (SK-N-AS, RTBM1, and SH-SY5Y) and reference DNA (normal female genomic DNA). Target DNAs were labeled with Cy3-dCTP and reference DNAs with Cy5-dCTP by random priming. Hybridization, scanning, and data processing were conducted as described previously [14,15].

Cell survival assays. Cells were plated at a density of 5000 cells/well in 96-well tissue culture plates. After attachment overnight, medium was replaced and treated with CDDP for 24 h. Cell viability was measured by MTT assay.

Flow cytometry. Floating and adherent cells were pooled and fixed in ice-cold 70% ethanol for 4 h at −20 °C. Cells were then stained with 10 mg/ml of PI (Sigma) in the presence of 250 mg/ml of RNase A at 37 °C for 30 min in the dark. Number of cells with sub-G1 DNA content was measured by flow cytometry (FACScan, Becton–Dickinson).

TUNEL assay. Apoptotic cells were identified using an *in situ* cell detection, peroxidase kit (Roche Applied Science). Briefly, cells were fixed in 4% paraformaldehyde and permeabilized with 0.1% Triton X-100. The labeling reaction was performed using TMR red-labeled dUTP together with other nucleotides by terminal deoxynucleotidyl transferase for 1 h in the dark at 37 °C. Then, cells were mounted and the incorporated TMR red-labeled dUTP was analyzed using a Fluoview laser scanning confocal microscope (Olympus).

Luciferase reporter assay. H1299 cells were co-transfected with pcDNA3, FLAG-p53 or FLAG-p53ΔC expression plasmid, p53-responsive luciferase reporter (*p21^{WAF1}*, *MDM2* or *Bax*), and pRL-TK *Renilla* luciferase cDNA. Forty-eight hours after transfection, firefly and *Renilla* luciferase activities were measured with dual-luciferase reporter assay system according to the manufacturer's instructions (Promega).

Colony formation assay. Forty-eight hours after transfection, SK-N-AS cells were transferred to fresh medium containing G418 (400 μg/ml). After 16 days of selection, drug-resistant colonies were fixed in methanol and stained with Giemsa's solution.

Results

DNA-damage response in human neuroblastoma cells

To determine the effects of genotoxic agents on neuroblastomas, human neuroblastoma SH-SY5Y and SK-N-AS cells were exposed to cisplatin (CDDP) and their viabilities were examined by MTT assays. As shown in Fig. 1A, their viabilities were significantly decreased in response to CDDP. To address whether CDDP could induce apoptosis, we performed TUNEL assay. As shown in Fig. 1B, we observed a higher number of TUNEL-positive SH-SY5Y cells exposed to CDDP, whereas CDDP had undetectable effects on SK-N-AS cells. We further determined apoptotic cells as sub-G1 population by flow cytometry. As seen in Fig. 1C, a significant increase in number of SH-SY5Y cells with sub-G1 DNA content was observed after CDDP treatment, whereas CDDP treatment of SK-N-AS cells resulted in an increase in S-phase cells but not in G2/M-phase cells. Consistent with these results, *thymidine kinase* (S-phase marker) [16] was increased in CDDP-treated SK-N-AS cells, whereas *Plk1* (M-phase marker) [17] remained unchanged regardless of CDDP treatment (data not shown).

We then examined whether p53-dependent apoptotic pathway could be activated in response to CDDP. As shown in Fig. 1D, p53 was phosphorylated at Ser-15 in SH-SY5Y cells exposed to CDDP. *p53* remained unchanged regardless of CDDP treatment, whereas p53 target genes including *p21^{WAF1}*, *Bax*, and *PUMA* were transactivated in response to CDDP. In contrast, CDDP-mediated phosphorylation of p53 at Ser-15 was undetectable in SK-N-AS cells. *p21^{WAF1}* was induced in response to CDDP, however, CDDP-mediated up-regulation of pro-apoptotic *Bax* and *PUMA* was undetectable, suggesting that p53 pro-apoptotic function might be lost in SK-N-AS cells.

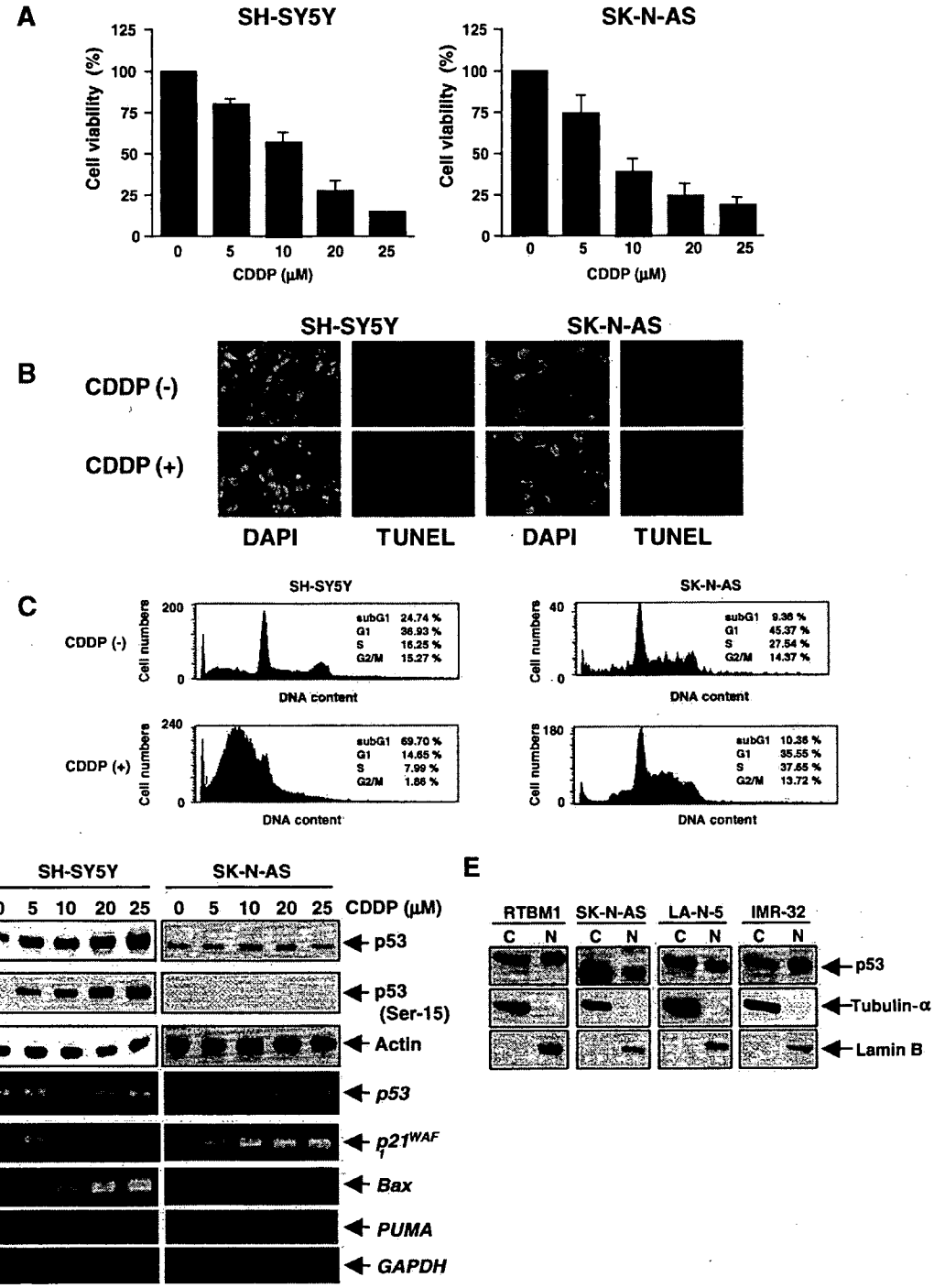

Fig. 1. Differential effects of CDDP on neuroblastoma cells. (A) Cell survival assays. Twenty-four hours after CDDP treatment, cell viability was analyzed by MTT assays. (B) TUNEL staining. Twenty-four hours after CDDP treatment (20 μM), apoptotic cells were detected by TUNEL staining. Cell nuclei were stained with DAPI. (C) FACS analysis. SH-SY5Y and SK-N-AS cells were treated as in (B). Twenty-four hours after CDDP treatment, cell cycle distributions were analyzed by FACS. Shown are the representatives of three independent experiments. (D) CDDP-induced accumulation of p53 in neuroblastoma cells. Twenty-four hours after CDDP treatment, lysates and total RNA were subjected to immunoblotting (upper panels) and RT-PCR (lower panels), respectively. For protein loading control, actin levels were checked by immunoblotting. For RT-PCR, *GAPDH* was used as a loading control. (E) Subcellular localization of p53. The indicated neuroblastoma cells were fractionated into cytoplasmic (C) and nuclear (N) fractions and subcellular distribution of p53 was analyzed by immunoblotting. Tubulin-α and Lamin B were used as cytoplasmic and nuclear markers, respectively.

To investigate molecular mechanism(s) behind p53 dysfunction in SK-N-AS cells, we examined subcellular localization of p53 in various neuroblastoma cells. As shown in Fig. 1E, p53 was detected in cytoplasm and nucleus of RTBM1, LA-N-5, and IMR-32 cells bearing wild-type *p53* (data not shown). Of note, p53 was abundantly expressed in cytoplasm of SK-N-AS cells and its molecular mass was smaller than those of other

cells, indicating that it might be due to certain structural aberrations.

Structural aberration of p53 in SK-N-AS cells

To address whether p53 could have any aberrations in SK-N-AS cells, we amplified the indicated genomic regions of *p53* using genomic DNA from SK-N-AS cells. RTBM1 cells were used as a positive control. As shown in Fig. 2A, PCR-based amplification using primer sets including P1, P2, P6, and P7 successfully generated estimated sizes of PCR products, whereas remaining primer sets (P3–P5) did not, suggesting that the genomic region containing exons 10 and 11 of *p53* might be lost in SK-N-AS cells.

To confirm genomic aberrations within *p53* locus in SK-N-AS cells, we performed Southern analysis. Radio-labeled *p53* cDNA probe failed to detect *Pst*I fragment (2.0 kb in length) which contains exons 10 and 11 in SK-N-AS cells (Fig. 2B). Our array-based comparative genomic hybridization (CGH) analysis demonstrated that there exists a large range of allelic deletion of chromosome 17p where *p53* is located in SK-N-AS cells (Fig. 2C). Furthermore, anti-p53 antibody which recognizes p53 extreme COOH-terminal portion could not detect p53 in SK-N-AS cells (Fig. 2D). Collectively, our results suggest that p53 COOH-terminal region is homozygously deleted in SK-N-AS cells. We then cloned *p53* cDNA. As shown in Fig. 2E, a newly identified p53 (p53ΔC) was composed of 369 amino acids including unique COOH-terminal structure (estimated molecular mass of 49 kDa), lacked a part of oligomerization domain, and completely lost NLS II and III. The 3′-side of intron 9 and the downstream region containing exons 10 and 11 were deleted in SK-N-AS cells. Its unique COOH-terminal amino acids were derived from intron 9, suggesting that accurate splicing event might be abrogated and thereby generating p53ΔC.

Dysfunction of p53ΔC

To ask whether p53ΔC could have functional differences as compared with wild-type p53, FLAG-p53 or FLAG-p53ΔC was expressed in SK-N-AS cells and their subcellular localization was examined. As shown in Fig. 3A, FLAG-p53 was detectable in cytoplasm and nucleus,

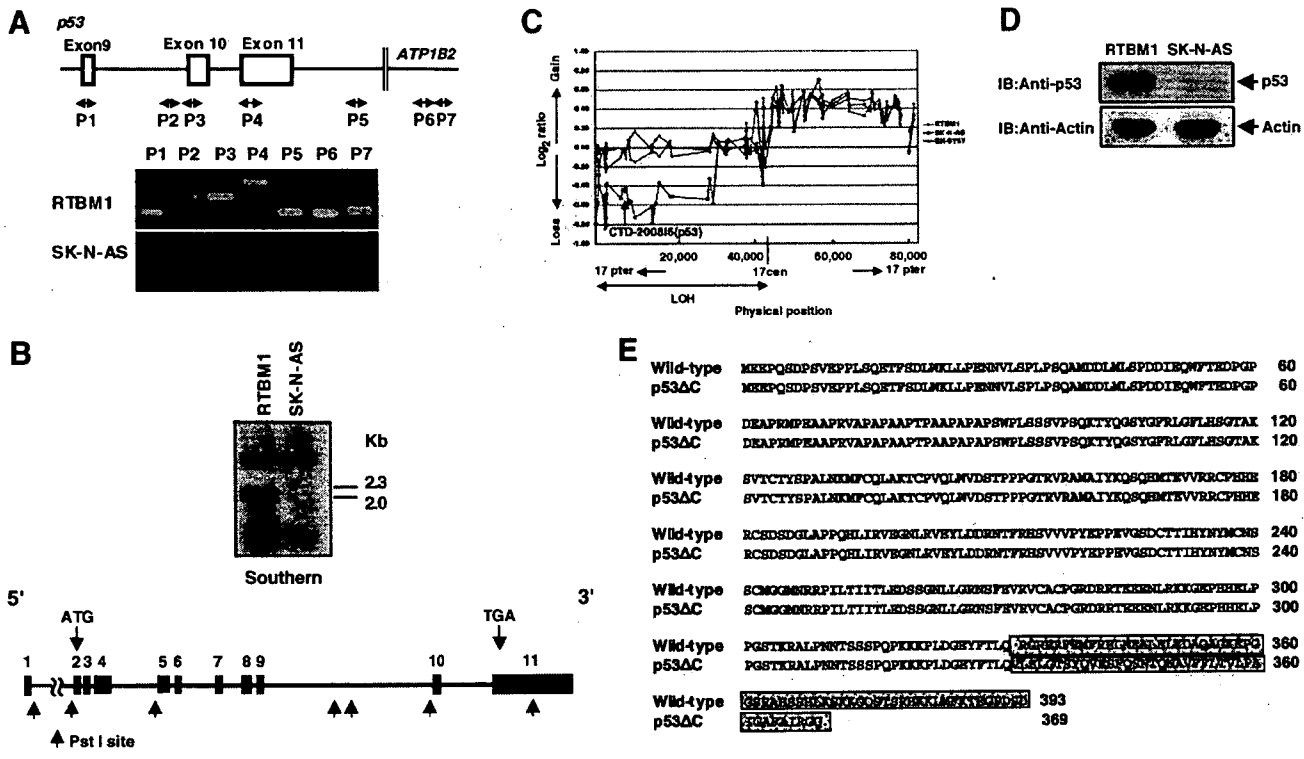

Fig. 2. p53 COOH-terminal region is deleted in SK-N-AS cells. (A) Genomic structure of human *p53* locus and positions of PCR primers (P1–P7) are shown. *ATP1B2* encodes ATPase, Na^+/K^+ transporting β2 (upper panel). Genomic DNA from RTBM1 and SK-N-AS cells was subjected to PCR using the indicated primers (lower panels). (B) Southern blot analysis. Genomic DNA was digested with *Pst*I, separated by 1% agarose gel, transferred onto nylon membrane, and probed with the radio-labeled *p53* cDNA. Schematic diagram of human *p53* and positions of *Pst*I sites are also shown. (C) Array-based comparative genomic hybridization (CGH) analysis. Hybridization was performed as described under Materials and methods. Arrays were scanned and images processed using custom software. We normalized relative ratios of tumor and normal signals by setting the value of the median relative ratio equal to 1. The data were then transformed into log 2 space and plotted as a histogram to determine cutoffs for scoring loss or gain. Three Gaussian distribution curves were fitted to the histogram, and values >3 SD from the central Gaussian were scored as losses or gains for that tumor. (D) Immunoblotting. Lysates from RTBM1 and SK-N-AS were processed for immunoblotting with the specific antibody against p53 extreme COOH-terminal portion. (E) Amino acid sequence alignment of wild-type p53 and p53ΔC. The different amino acid residues between them are boxed.

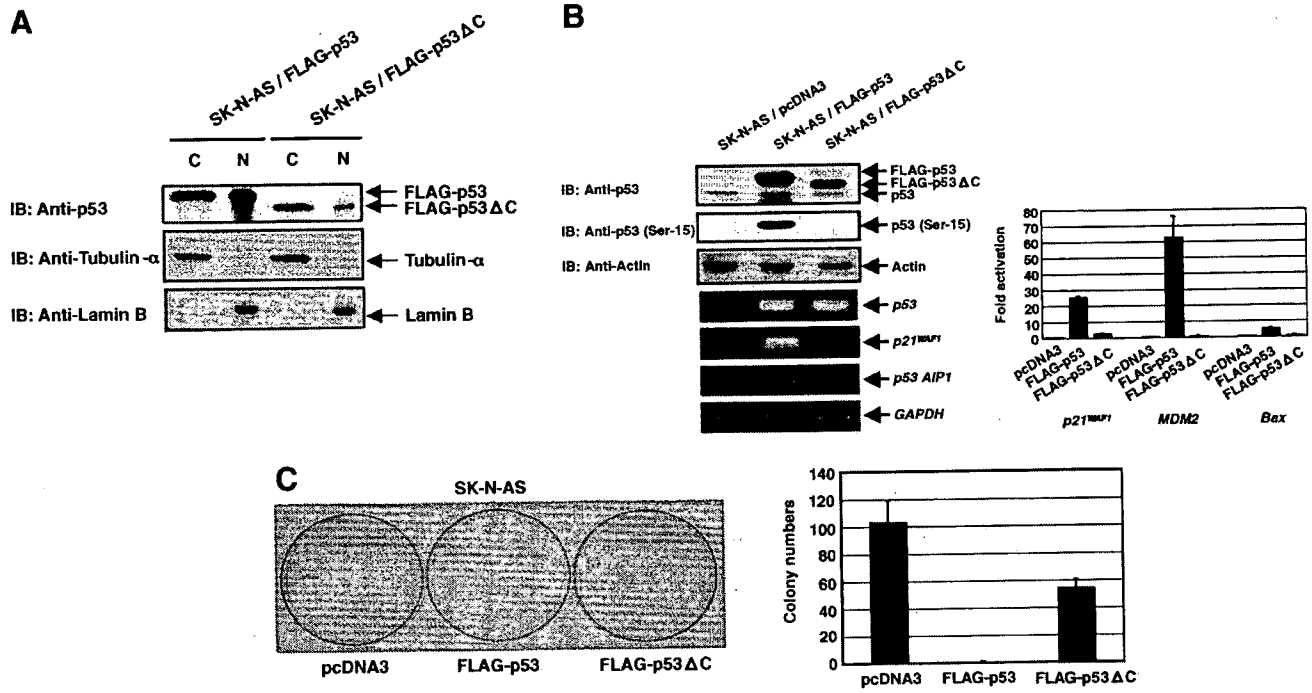

Fig. 3. Loss of function of p53ΔC. (A) Subcellular localization of exogenously expressed wild-type p53 and p53ΔC. SK-N-AS cells were transfected with the indicated expression plasmids. Forty-eight hours after transfection, cells were fractionated into cytoplasmic (C) and nuclear (N) fractions followed by immunoblotting with anti-p53 antibody. (B) Possible effects of COOH-terminal deletion of p53 on its transcriptional activity. SK-N-AS cells were transfected with the indicated expression plasmids. Forty-eight hours after transfection, lysates and total RNA were subjected to immunoblotting and RT-PCR, respectively (left panel). (Right panel) Luciferase reporter assays. *p53*-deficient H1299 cells were co-transfected with pcDNA3, FLAG-p53 or FLAG-p53ΔC expression plasmid, p53-responsive luciferase reporter (*$p21^{WAF1}$*, *MDM2* or *Bax*) and *Renilla* luciferase cDNA. Forty-eight hours after transfection, luciferase activities were measured. (C) Colony formation assay. Forty-eight hours after transfection, SK-N-AS cells were transferred to fresh medium containing G418 (400 μg/ml). Sixteen days after selection with G418, drug-resistant colonies were stained with Giemsa's solution (left panel) and the number of colonies was scored (right panel).

whereas FLAG-p53ΔC was largely expressed in cytoplasm. Next, we examined transcriptional potential of p53ΔC in SK-N-AS cells. As seen in left panel of Fig. 3B, FLAG-p53 but not FLAG-p53ΔC was phosphorylated at Ser-15. Consistent with these results, FLAG-p53 transactivated *$p21^{WAF1}$* and *p53AIP1*. In contrast, FLAG-p53ΔC failed to transactivate *$p21^{WAF1}$* and *p53AIP1*. Similar results were also obtained by luciferase reporter assays (Fig. 3B, right panel). To examine effects of COOH-terminal deletion on pro-apoptotic activity of p53, we performed colony formation assays. SK-N-AS cells were transfected with empty plasmid, FLAG-p53 or FLAG-p53ΔC expression plasmid and maintained in medium containing G418 for 16 days. As shown in Fig. 3C, number of drug-resistant colonies was significantly reduced in cells expressing FLAG-p53. Intriguingly, enforced expression of FLAG-p53ΔC resulted in a decrease in number of drug-resistant colonies but to a lesser degree as compared with that in cells expressing FLAG-p53. These observations suggest that COOH-terminal deletion reduces transcriptional and pro-apoptotic activities of p53.

Discussion

In this study, we have identified p53ΔC in SK-N-AS cells. Consistent with the recent report [13], p53 was predominantly expressed in cytoplasm of SK-N-AS cells. According to their results, Parc inhibited p53 nuclear translocation through the direct interaction with its COOH-terminal region. Since p53 contains three NLSs in its COOH-terminal region, Parc might inhibit its nuclear access by masking its NLSs [13]. In accordance with these findings, p53 COOH-terminal peptide inhibited its cytoplasmic retention [12]. Based on our immunoprecipitation experiments, wild-type p53 but not p53ΔC was co-immunoprecipitated with the endogenous Parc in SK-N-AS cells (data not shown), suggesting that cytoplasmic retention of p53ΔC is regulated in a Parc-independent manner. p53ΔC lacks NLS II and III but retains NLS I. Although Kim et al. described that importin-α interacts with NLS I of p53 and mediates its nuclear import [18], NLS II and/or III might play a major role in nuclear import of p53 in SK-N-AS cells.

p53 phosphorylation is significantly associated with its pro-apoptotic function [4]. Exogenously expressed wild-type p53 but not p53ΔC was phosphorylated at Ser-15 in SK-N-AS cells without DNA damage and transactivated *$p21^{WAF1}$* and *p53AIP1*. Rodicker and Putzer described that exogenously expressed p53 is phosphorylated at Ser-15 without DNA damage [19]. Although it is unknown why exogenously expressed p53 but not p53ΔC is phosphorylated at Ser15 without DNA damage, it might be at least

in part due to its cytoplasmic retention. Colony formation assays demonstrated that wild-type p53 markedly reduces number of drug-resistant colonies in SK-N-AS cells, suggesting that there might not exist functional disruptions of downstream mediators of p53 in SK-N-AS cells. In response to CDDP, SH-SY5Y cells underwent apoptosis in association with a significant induction of p53. On the other hand, SK-N-AS cells did not undergo apoptosis in response to CDDP, suggesting that *p53* status might determine neuroblastoma cell fate to survive or to die. Intriguingly, CDDP treatment of SK-N-AS cells induced an accumulation of S-phase cells accompanied with up-regulation of $p21^{WAF1}$. Since p53ΔC failed to transactivate $p21^{WAF1}$ and CDDP had undetectable effects on *p73* and *p63* (other members of *p53* family) (data not shown), CDDP-mediated up-regulation of $p21^{WAF1}$ in SK-N-AS cells is regulated in a p53 family-independent manner. Knudsen et al. reported that CDDP-mediated DNA damage induces an intra-S-phase cell cycle arrest, which is correlated with a protection against apoptosis [20]. Thus, the genome maintenance system might delay the onset of mitosis, and thereby providing time to complete DNA repair and/or DNA replication before cell division in SK-N-AS cells. Further efforts should be necessary to address this issue.

Majority of *p53* mutations is detected within its DNA-binding region [21]. SK-N-AS cells have been believed to express wild-type p53 [22]. Much of information regarding *p53* mutations was derived from sequence analysis of exons 5–8 which encode its DNA-binding domain [4]. Indeed, there exist missense mutations in p53 oligomerization domain [23]. According to their results, Leu to Pro substitution at 344 inhibited the oligomerization of p53 and abolished its DNA-binding activity. Since p53ΔC lacks a part of oligomerization domain including Leu-344, p53ΔC might exist as a monomeric latent form. Recently, Bourdon et al. described that human *p53* is expressed as multiple isoforms including p53β and p53γ [24]. Based on amino acid sequence comparison, p53ΔC was distinct from p53β and p53γ (data not shown). During the preparation of our manuscript, Goldschneider et al. reported that SK-N-AS cells express p53β [25]. This discrepancy might be attributed to co-expression of p53β and p53ΔC in SK-N-AS cells and/or due to the acquired heterogeneity of SK-N-AS cells during culture. Additionally, murine *p53* expresses an alternative splicing isoform termed ASp53 with different COOH-terminus from that of wild-type p53 [26]. ASp53 displays an enhanced transcriptional activity as compared with wild-type p53, indicating that p53ΔC is distinct from human counterpart of ASp53.

Acknowledgments

This work was supported in part by a Grant-in-Aid from the Ministry of Health, Labor and Welfare for Third Term Comprehensive Control Research for Cancer, a Grant-in-Aid for Scientific Research on Priority Areas from the Ministry of Education, Culture, Sports, Science and Technology, Japan, a Grant-in-Aid for Scientific Research from Japan Society for the Promotion of Science, and a Grant from Uehara Memorial Foundation.

References

[1] M. Hollstein, D. Sidransky, B. Vogelstein, H. Harris, p53 mutations in human cancers, Science 253 (1991) 49–53.
[2] A.J. Levine, J. Momand, C.A. Finlay, The p53 tumour suppressor gene, Nature 351 (1991) 453–456.
[3] L.A. Donehower, M. Harvey, B.L. Slagle, M.J. McArthur, C.A. Montgomery Jr., J.S. Butel, A. Bradley, Mice deficient for p53 are developmentally normal but susceptible to spontaneous tumours, Nature 356 (1992) 215–221.
[4] K.H. Vousden, X. Lu, Live or let die: the cells response to p53, Nat. Rev. Cancer 2 (2002) 594–604.
[5] Y. Haupt, R. Maya, A. Kazaz, M. Oren, Mdm2 promotes the rapid degradation of p53, Nature 387 (1997) 296–299.
[6] M.H.G. Kubbutat, S.N. Jones, K.H. Vousden, Regulation of p53 stability by Mdm2, Nature 387 (1997) 299–303.
[7] G. Shaulsky, N. Goldfinger, A. Ben-Ze'ev, V. Rotter, Nuclear accumulation of p53 protein is mediated by several nuclear localization signals and plays a role in tumorigenesis, Mol. Cell. Biol. 10 (1990) 6565–6577.
[8] S.H. Liang, D. Hong, M.F. Clarke, Cooperation of a single lysine mutation and a C-terminal domain in the cytoplasmic sequestration of the p53 protein, J. Biol. Chem. 273 (1998) 19817–19821.
[9] K. Vogan, M. Bernstein, J.M. Leclerc, L. Brisson, J. Brossard, G.M. Brodeur, J. Pelletier, P. Gros, Absence of p53 gene mutations in primary neuroblastomas, Cancer Res. 53 (1993) 5269–5273.
[10] U.M. Moll, M. LaQuaglia, J. Benard, G. Riou, Wild-type p53 protein undergoes cytoplasmic sequestration in undifferentiated neuroblastomas but not in differentiated tumors, Proc. Natl. Acad. Sci. USA 92 (1995) 4407–4411.
[11] U.M. Moll, A.G. Ostermeyer, R. Haladay, B. Winkfield, M. Frazier, G. Zambetti, Cytoplasmic sequestration of wild-type p53 protein impairs the G1 checkpoint after DNA damage, Mol. Cell. Biol. 16 (1996) 1126–1137.
[12] A.G. Ostermeyer, E. Runko, B. Winkfield, B. Ahn, U.M. Moll, Cytoplasmically sequestrated wild-type p53 protein in neuroblastoma is relocated to the nucleus by a C-terminal peptide, Proc. Natl. Acad. Sci. USA 93 (1996) 15190–15194.
[13] A.Y. Nikolaev, M. Li, N. Puskas, J. Qin, W. Gu, Parc: A cytoplasmic anchor for p53, Cell 112 (2003) 29–40.
[14] A.M. Snijders, N. Nowak, R. Segraves, S. Blackwood, N. Brown, J. Conroy, G. Hamilton, A.K. Hindle, B. Huey, K. Kimura, S. Law, K. Myambo, J. Palmer, B. Yistra, J.P. Yue, J.W. Gray, A.N. Jain, D. Pinkel, D.G. Albertson, Assembly of microarrays for genome-wide measurement of DNA copy number, Nat. Genet. 29 (2001) 263–264.
[15] J.M. Nigro, A. Misra, L. Zhang, I. Smimov, H. Colman, C. Griffin, N. Ozburn, M. Chen, E. Pan, D. Koul, W.K. Yung, B.G. Feuerstein, K.D. Aldape, Integrated array-comparative genomic hybridization and expression array profiles identity clinically relevant molecular subtypes of glioblastoma, Cancer Res. 65 (2005) 1678–1686.
[16] D.L. Coppock, A.B. Pardee, Control of thymidine kinase mRNA during the cell cycle, Mol. Cell. Biol. 7 (1987) 2925–2932.
[17] R. Hamanaka, M.R. Smith, P.M. O'Connor, S. Maloid, K. Mihalic, J.L. Spivak, D.L. Longo, D.K. Ferris, Polo-like kinase is a cell cycle-regulated kinase activated during mitosis, J. Biol. Chem. 270 (1995) 21086–21091.
[18] I.S. Kim, D.H. Kim, S.M. Han, M.U. Chin, H.J. Nam, H.P. Cho, S.Y. Choi, B.J. Song, E.R. Kim, Y.S. Bae, Y.H. Moon, Truncated form of importin α identified in breast cancer cell inhibits nuclear import of p53, J. Biol. Chem. 275 (2000) 23139–23145.

[19] F. Rodicker, B.M. Putzer, p73 is effective in p53-null pancreatic cancer cells resistant to wild-type TP53 gene replacement, Cancer Res. 63 (2003) 2737–2741.
[20] K.E. Knudsen, D. Booth, S. Naderi, Z. Sever-Chroneos, A.F. Fribourg, C. Hunton, J.R. Feramisco, J.Y.J. Wang, E.S. Knudsen, RB-dependent S-phase response to DNA damage, Mol. Cell. Biol. 20 (2000) 7751–7763.
[21] M. Hollstein, M. Hergenhahn, Q. Yang, H. Bartsch, Z.Q. Wang, P. Hainaut, New approaches to understanding p53 gene tumor mutation spectra, Mutat. Res. 431 (1999) 199–209.
[22] M. Kaghad, H. Bonnet, A. Yang, L. Creancier, J.C. Biscan, A. Valent, A. Minty, P. Chalon, J.M. Lelias, X. Dumont, P. Ferrara, F. McKeon, D. Caput, Monoallelically expressed gene related to p53 at 1p36, a region frequently deleted in neuroblastoma and other human cancers, Cell 90 (1997) 809–819.
[23] M.E. Lomax, D.M. Barnes, T.R. Hupp, S.M. Picksley, R.S. Camplejohn, Characterization of p53 oligomerization domain mutations isolated from Li-Fraumeni and Li-Fraumeni like family members, Oncogene 17 (1998) 643–649.
[24] J.C. Bourdon, K. Fernandes, F. Murray-Zmijewski, G. Liu, A. Diot, D.P. Xirodimas, M.K. Saville, D.L. Lane, p53 isoforms can regulates p53 transcriptional activity, Genes Dev. 19 (2005) 2122–2137.
[25] D. Goldschneider, E. Horvilleur, L.F. Plassa, M. Guillaud-Bataille, K. Million, E. Wittmer-Dupret, G. Danglot, H. de The, J. Benard, E. May, S. Douc-Rasy, Expression of C-terminal deleted p53 isoforms in neuroblastoma, Nucleic Acids Res. 34 (2006) 5603–5612.
[26] N. Arai, D. Nomura, K. Yokota, D. Wolf, E. Brill, O. Shohat, V. Rotter, Immunologically distinct p53 molecules generated by alternative splicing, Mol. Cell. Biol. 6 (1986) 3232–3239.

Purification of human primary neuroblastomas by magnetic beads and their *in vitro* culture

HIROKO NAKANISHI[1,2], TOSHINORI OZAKI[1], YOUKO NAKAMURA[1], KOHEI HASHIZUME[3], TADASHI IWANAKA[2] and AKIRA NAKAGAWARA[1]

[1]Division of Biochemistry, Chiba Cancer Center Research Institute, 666-2 Nitona, Chuoh-ku, Chiba 260-8717; [2]Department of Pediatric Surgery, Graduate School of Medicine, University of Tokyo, 7-3-1 Hongo, Bunkyo-ku, Tokyo 113-0033; [3]Tokyo-West Tokushukai Hospital, 3-1-1 Matsubara-cho, Akishima 196-0003, Japan

Received January 2, 2007; Accepted February 20, 2007

Abstract. In the present study we have successfully isolated neuroblastoma cells from primary human neuroblastoma tissues by using a magnetic bead-mediated purification system. Since primary neuroblastoma tissues contained CD3- and CD19-positive lymphocytes, total cell suspensions were prepared and incubated with magnetic beads coated with anti-CD3 or with anti-CD19 antibody. After magnetic separation, unbound materials were recovered and analyzed by immunohistochemical staining for NB84, one of the neuroblastoma markers. Immunohistochemical and FACS analyses demonstrated that NB84-positive cells were enriched in the unbound fraction. Subsequently, unbound materials were seeded on cell culture plates and maintained at 37°C overnight. After incubation, non-adherent cells were collected and stained with anti-NB84 antibody. Under our experimental conditions, a significant increase in the number of NB84-positive cells was observed. Furthermore, our purified NB84-positive cells responded to all-*trans* retinoic acid and nerve growth factor better than the initial primary cells. Collectively, our present results suggest that magnetic bead-mediated purification enriches neuroblastoma cells which retain their biological properties.

Introduction

Neuroblastoma is one of the most common early childhood solid tumors of the peripheral nervous system arising from an as yet unidentified population of neural crest cells (1), and is clinically and cytogenetically divided into two major subgroups with distinct biological properties (2). One subgroup of tumors in the early stages displays favorable prognosis and usually occurs in patients <1 year of age. They have no *MYCN* gene amplification and often differentiate and/or regress spontaneously. In sharp contrast, tumors that occur in patients >1 year of age usually possess *MYCN* gene amplification and allelic loss in the distal part of the short arm of chromosome 1, and are often aggressive with an unfavorable prognosis in spite of an intensive multimodal therapy (3). Additionally, it has been shown that high expression levels of neurotrophin receptor genes *TrkA* and *TrkB* are favorable and unfavorable prognostic indicators, respectively (4-6). However, the precise molecular mechanisms behind disease progression and tumor regrowth are still unclear. From a clinical point of view, aggressive neuroblastomas are the most problematic, and it is quite difficult to decide which therapeutic strategy is suitable.

As described previously (7), neuroblastomas exhibit heterogenous morphologies with tumors composed of a mixture of neuroblasts, ganglion cells, non-neuronal Schwann-like cells and stromal cells. Indeed, human neuroblastoma-derived cell lines consist of heterogenous subpopulations of cells which show distinct morphological and biochemical features (7-10). The established neuroblastoma cell lines spontaneously give rise to diverse populations of neuroblastic (N-type) and Schwann-like (S-type) cells (9,10). In addition to N- and S-type cells, cells with intermediate morphology (I-type) have also been cloned (11), and these three subtypes have an ability to interconvert or transdifferentiate spontaneously (12), suggesting that N-type to S-type differentiation might reflect *in vivo* differentiation of the tumor. To better understand the biological behavior as well as molecular events *in vivo*, it seems to be important to remove the additional components such as non-neuronal Schwann-like and stromal cells from neuroblastomas in culture.

In the present study, we have obtained successful results isolating neuroblastoma cells from primary neuroblastoma tissues by using magnetic bead-mediated purification.

Materials and methods

Patient population. Tumors were staged following the International Neuroblastoma Staging System criteria (13).

Correspondence to: Dr Akira Nakagawara, Division of Biochemistry, Chiba Cancer Center Research Institute, 666-2 Nitona, Chuoh-ku, Chiba 260-8717, Japan
E-mail: akiranak@chiba-cc.jp

Key words: NB84, neuroblastoma, nerve growth factor, retinoic acid

The patients were treated according to the protocols proposed by the Japanese Infantile Neuroblastoma Cooperative Study (14) and the Study Group of Japan for Treatment of Advanced Neuroblastoma (15). All patients agreed to participate and provided written informed consent. Our present study was approved by the institutional ethics review committee.

Primary culture. Fresh human neuroblastoma tissues were minced and incubated with RPMI-1640 medium supplemented with 10% heat-inactivated fetal bovine serum, penicillin (50 U/ml), streptomycin (50 μg/ml) and 100 μg/ml of OPI (Sigma, St. Louis, MO, USA) in the presence of 500 units/ml of collagenase (Sigma) at 37°C for 1 h. After incubation, tumor tissues were dispersed by using a plastic syringe with an 18-gauge needle, seeded on tissue culture plates precoated with collagen, and cultured at 37°C with 5% CO_2 in a humidified incubator. Where indicated, cells were treated with the indicated combinations of all-*trans* retinoic acid (ATRA, Sigma) and nerve growth factor (NGF, Sigma), and their effects on neurite outgrowth were examined with a phase-contrast microscope.

Purification of neuroblastoma tumors. The magnetic beads were conjugated with anti-mouse IgG. After incubation, the magnetic beads (Dynal, Oslo, Norway) were washed in PBS and then incubated for 4-8 h with monoclonal anti-CD3 (DHCT1, Ancell, Bayport, MN) or with anti-CD19 (BU12, Ancell) antibody at 4°C. The indicated beads were mixed and incubated for 1 h at 4°C with cell suspensions before magnetic separation to isolate the two fractions: cells bound to the beads (lymphocytes) versus cells not bound to the beads (neuroblastomas, Schwann cells and fibroblasts). The latter cell fraction was subsequently cultured in a standard medium overnight at 37°C, and then separated into adherent cells (Schwann cells and fibroblasts) and non-adherent cells (neuroblastomas).

Measurement of cell viability. The trypan blue dye exclusion experiments were carried out by incubating the cell suspension with an equal amount of 0.3% trypan blue solution (Sigma) for 5 min at room temperature. After the incubation, the number of cells excluding trypan blue was measured by using a hemocytometer to estimate the number of intact viable cells.

Immunohistochemistry. Neuroblastoma tissues were fixed in 10% formaldehyde, embedded in paraffin, and 3-μm sections were subjected to immunostaining. Before incubating with anti-NB84 antibody (NB84a, Novocastra Laboratories, Newcastle, UK), the sections were treated with 0.05% Pronase in 50 mM Tris-HCl (pH 7.5) for 5 min. The sections were stained with anti-NB84 antibody at 4°C overnight, processed for the biotin-streptavidin method (Nichirei, Tokyo, Japan), and visualized with diaminobenzidine solution. Cell nuclei were stained with hematoxylin and eosin (H&E).

Flow cytometry. Cells (3-5x10^5) were washed in ice-cold PBS, and fixed in 0.25% paraformaldehyde for 15 min at room temperature. After washing in PBS, cells were incubated with anti-CD3 or with anti-CD19 antibody followed by incubation with FITC-conjugated isotype-specific secondary antibody (Invitrogen, Carlsbad, CA) at 4°C for 30 min. After washing in PBS, analysis was performed by FACS flow cytometer (Becton Dickinson, San Diego, CA). Cells were properly gated and histograms [FITC-fluorescence (x-axis) versus counts (y-axis)] were plotted to illustrate the logarithmic fluorescence intensity.

Results

Immunohistochemical analysis of human primary neuroblastomas. The 52 examined fresh human primary neuroblastoma samples were divided into 38 non-disseminated tumors with excellent outcome (stage 1, 2 and 4s) and 14 disseminated tumors with unfavorable outcome (stage 3 and 4). These primary samples were subjected to primary cultures according to a standard protocol, and their viability was examined by trypan blue dye exclusion assay. Under our experimental conditions, 91 and 94% of non-disseminated and disseminated cells were viable, respectively (data not shown). In accordance with recent observations (16), the represented immunohistochemical analysis revealed that surgically resected tumor tissues (case 625) contained NB84-positive neuroblastoma cells as well as lymphocytes, fibroblasts and Schwann cells (Fig. 1A). Similar results were also obtained in immunohistochemical analysis of total cell suspensions prepared from case 625 (Fig. 1B). NB84 has been considered to be one of the neuroblastoma markers (17).

Purification of neuroblastoma cells by using magnetic beads. To examine the amounts of lymphocytes included in primary neuroblastoma samples, we performed FACS analysis. For this purpose, total cell suspensions prepared from 24 cases including 14 non-disseminated tumors and 10 disseminated tumors were incubated with magnetic beads conjugated with anti-CD3 or with anti-CD19 antibody, and the unbound materials were again subjected to the magnetic bead treatment. Then unbound materials were processed for FACS analysis to determine the number of CD3- or CD19-positive cells. The representative data (case 625) are shown in Fig. 2A. Total cell suspensions contained 41% CD3-positive cells (T cells) but no CD19-positive cells (B cells). As expected, magnetic bead treatment resulted in a complete removal of CD3-positive cells. The cell viability of the bound materials (lymphocyte fractions) derived from non-disseminated and disseminated tumors was 81 and 79%, respectively (data not shown). On the other hand, the cell viability of the unbound materials prepared from non-disseminated and disseminated tumors was 94 and 92%, respectively (data not shown). We then examined the unbound materials by immunohistochemical analysis. As shown in Fig. 2B, NB84-positive cells were relatively enriched after magnetic bead-mediated separation. The unbound materials still contained NB84-positive neuroblastoma cells as well as fibroblasts and Schwann cells. According to our preliminary observations, neuroblastoma cells were less adherent than Schwann cells as well as fibroblasts to culture plates (data not shown). To separate NB84-positive neuroblastoma cells from fibroblasts and Schwann cells, the unbound materials were seeded on cell culture plates and incubated at 37°C overnight. After incubation, non-adherent cells were recovered and subjected

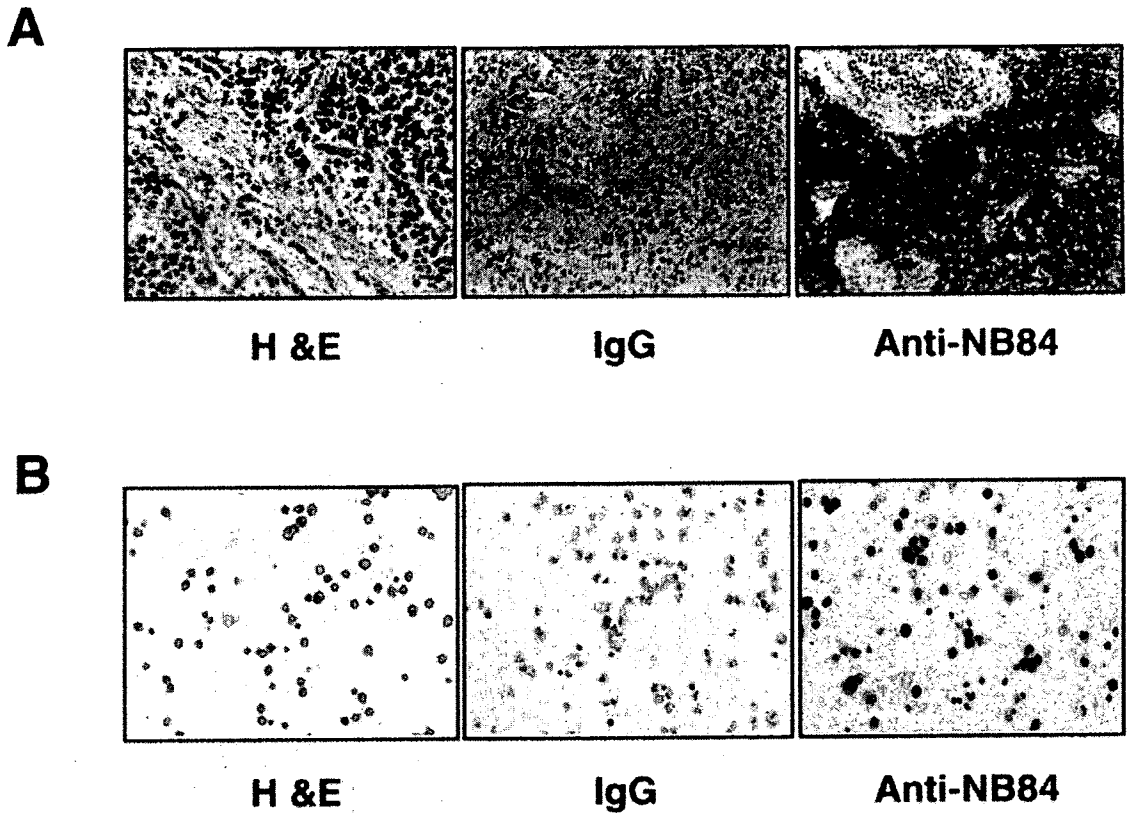

Figure 1. Immunohistochemical staining for NB84 in human primary neuroblastoma tissues. (A) Clinical samples of the patient with neuroblastoma (case 625) were subjected to H&E staining. Alternatively, these primary samples were processed for immunohistochemical staining with control IgG or with anti-NB84 antibody. (B) H&E and immunohistochemical staining of cell suspensions prepared from primary neuroblastoma (case 625).

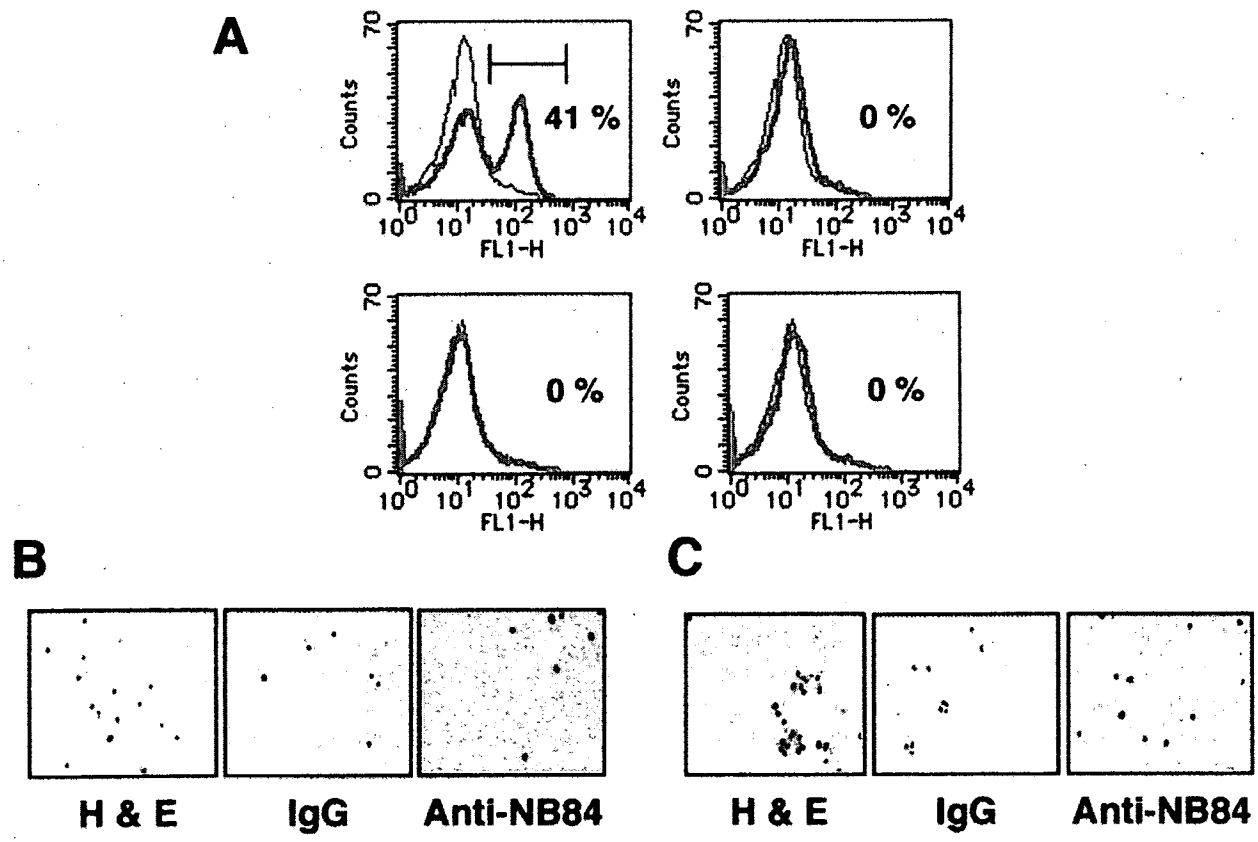

Figure 2. Flow cytometric analysis of primary neuroblastoma. (A) Total cell suspensions prepared from primary neuroblastoma (case 625) were analyzed by flow cytometry for the expression of CD3 and CD19 before and after magnetic separation. (B) Immunohistochemical analysis of neuroblastoma cell suspensions (case 625) after magnetic separation (CD3- and CD19-negative cells). (C) After magnetic separation of neuroblastoma cell suspensions (case 625), CD3- and CD19-negative cells were maintained overnight, and non-adherent cells were collected followed by immunohistochemical staining.

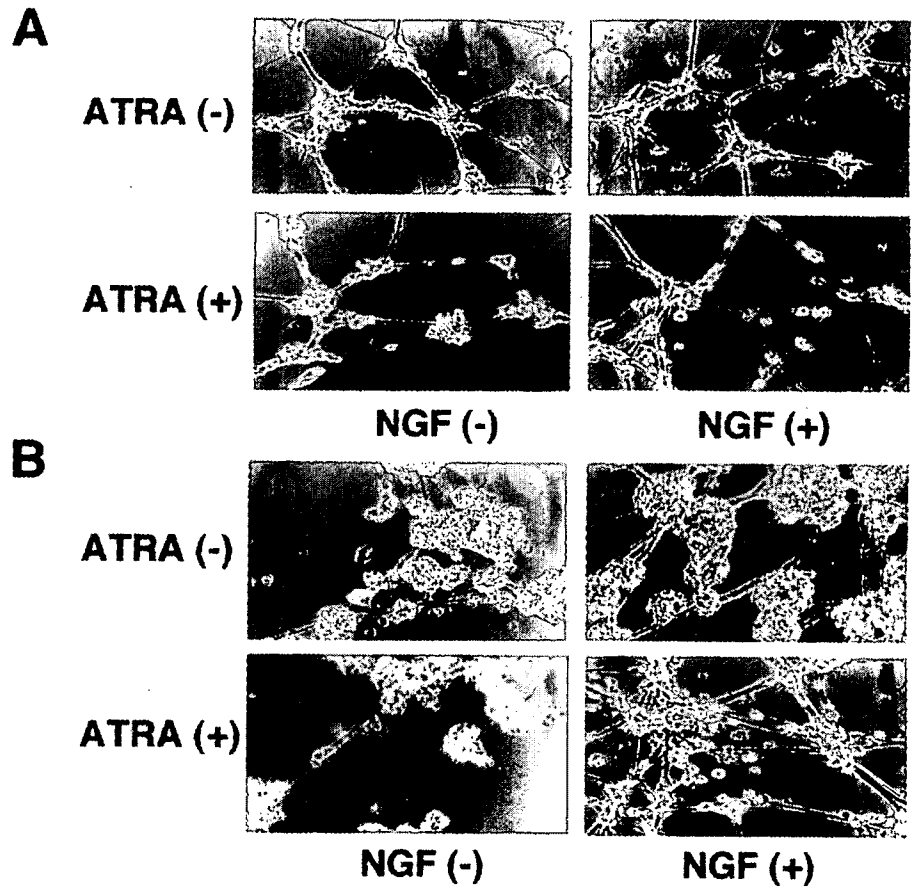

Figure 3. Neurite extension of primary neuroblastomas in response to NGF and/or ATRA. Total cell suspensions (A) and CD3- and CD19-negative non-adherent cells (B) prepared from case 625 were treated with or without the indicated combinations of NGF (100 ng/ml) and ATRA (5 μM) for seven days, and their neurite outgrowth was examined.

to immunohistochemical staining with anti-NB84 antibody. As shown in Fig. 2C, NB84-positive neuroblastoma cells were efficiently enriched by our present procedure.

Neurite extension in response to ATRA and/or NGF. To address whether magnetic bead-mediated enrichment of neuroblastoma cells could affect their biological behavior, we compared the degree of neurite outgrowth between cells before and after the selection. To this end, total cell suspensions and CD3- and CD19-negative non-adherent cells prepared from case 625 were cultured in the presence or absence of ATRA and/or NGF. Seven days after treatment, cells were observed with a phase-contrast microscope. Representative data are shown in Fig. 3A and B. ATRA alone had undetectable effects on both cells, whereas NGF treatment led to a formation of neurites in both cells. To note, treatment of CD3- and CD19-negative non-adherent cells with the combination of ATRA and NGF significantly enhanced neurite outgrowth as compared with total cell suspensions, suggesting that NB84-positive neuroblastoma cells purified by magnetic bead-mediated separation retain the biological properties of primary neuroblastomas.

Discussion

To understand the biological properties of neuroblastomas *in vivo*, it is necessary to isolate neuroblastoma cells from fresh neuroblastoma tissues in culture. As described previously (18), growth factors have an ability to promote proliferation or differentiation of neuroblastoma cells through interactions with their specific receptors. Among them, NGF, which induces normal adrenal cells to differentiate into cells identical to sympathetic neurons, plays a key role in the development of neuroblastomas (19). It has been well established that the high-affinity NGF receptor *TrkA* gene is highly expressed in low-stage neuroblastomas but not in advanced neuroblastomas (4). Several lines of evidence suggest that NGF responsiveness of neuroblastoma-derived cell lines is closely associated with the expression levels of *TrkA* and the low-affinity NGF receptor gene $p75^{NTR}$ (20,21). Since $p75^{NTR}$ alone had undetectable effects on NGF responsiveness of neuroblastoma cell lines (22), we sought to isolate neuroblastoma cells from primary neuroblastoma tissues by using magnetic beads coated with anti-$p75^{NTR}$ antibody. Under our experimental conditions, we failed to enrich neuroblastoma cells due to diverse expression levels of $p75^{NTR}$ in primary neuroblastoma samples (data not shown).

During the preparation of primary neuroblastoma samples, we noticed that primary neuroblastoma tissues contain substantial amounts of lymphocytes. We then employed magnetic beads coated with anti-CD3 or anti-CD19 antibody to remove lymphocytes from primary neuroblastoma samples. After magnetic separation, the unbound materials were cultured overnight and the non-adherent cells were collected.

Table I. FACS analysis of advanced neuroblastomas.

			Total cell suspension				Cells after treatment with beads		
			Lymphocytes			NB cells	Lymphocytes		NB cells
Case	Age	Stage	Total (%)	CD3 (%)	CD19 (%)	NB84 (%)	CD3 (%)	CD19 (%)	NB84 (%)
548	2 years	4	4	4	0	ND	ND	ND	ND
559	1 year	3	20	20	0	ND	0	0	ND
564	2 years	4	20	7	13	ND	0	0	ND
580	9 months	3	21	9	12	ND	ND	ND	ND
581	1 year	4	31	31	0	ND	ND	ND	ND
602	1 year	4	13	13	0	17	0	0	50
603	2 years	4	15	4	11	ND	ND	ND	ND
613	4 years	4	56	28	28	16	0	0	51
615	7 months	3	15	11	4	ND	0	0	ND
649	6 years	4	0	0	0	22	0	0	56

ND, not determined.

Table II. FACS analysis of neuroblastomas in stages 1, 2 and 4s.

			Total cell suspension				Cells after treatment with beads		
			Lymphocytes			NB cells	Lymphocytes		NB cells
Case	Age	Stage	Total (%)	CD3 (%)	CD19 (%)	NB84 (%)	CD3 (%)	CD19 (%)	NB84 (%)
601	9 months	2	28	20	8	ND	ND	ND	ND
609	7 months	1	58	44	14	ND	0	0	ND
611	7 months	4s	57	57	0	ND	0	0	ND
619	9 months	2	83	72	11	50	0	0	ND
624	8 months	1	96	48	48	ND	40	34	ND
625	7 months	1	41	41	0	66	0	0	72
627	7 months	1	15	15	0	0	0	0	ND
641	7 months	1	0	0	0	64	0	0	65
643	1 year	1	0	0	0	78	0	0	86
678	7 months	1	15	14	1	86	2	0	95
684	8 months	1	4	4	0	95	0	0	97
687	8 months	1	11	10	1	86	2	1	75
711	7 months	1	20	19	1	79	0	0	95
716	8 months	1	20	18	2	22	2	1	60

ND, not determined.

FACS analysis revealed that our procedure successfully enriches NB84-positive viable neuroblastoma cells (Tables I and II), indicating that NB84-positive neuroblastoma cells can be separated from Schwann cells as well as from fibroblasts by taking advantage of their differential adhesion. Moreover, NB84-positive neuroblastoma cells responded to ATRA and NGF, suggesting that our enriched materials retained the biological properties of primary neuroblastomas. Collectively, our magnetic bead-mediated isolation system provides fresh and enriched neuroblastoma cells in culture.

Acknowledgements

This study was supported in part by a Grant-in-Aid from the Ministry of Health, Labour and Welfare for Third Term Comprehensive Control Research for Cancer, a Grant-in-Aid for Scientific Research on Priority Areas from the Ministry of Education, Culture, Sports, Science and Technology, Japan, a Grant-in-Aid for Scientific Research from Japan Society for the Promotion of Science and Uehara Memorial Foundation.

References

1. Brodeur GM: Neuroblastoma: biological insights into a clinical enigma. Nat Rev Cancer 3: 203s216, 2003.
2. Schor NF: Neuroblastoma as a neurobiological disease. J Neurooncol 41: 159-166, 1999.
3. Brodeur GM and Nakagawara A: Molecular basis of clinical heterogeneity in neuroblastoma. Am J Pediatr Hematol Oncol 14: 111-116, 1992.
4. Nakagawara A, Arima-Nakagawara M, Scavarda NJ, Azar CG, Cantor AB and Brodeur GM: Association between high levels of expression of the TRK gene and favorable outcome in human neuroblastoma. N Engl J Med 328: 847-854, 1993.
5. Nakagawara A, Azar CG, Scavarda NJ and Brodeur GM: Expression and function of TRK-B and BDNF in human neuroblastomas. Mol Cell Biol 14: 759-767, 1994.
6. Brodeur GM, Nakagawara A, Yamashiro DJ, Ikegaki N, Liu XG, Azar CG, Lee CP and Evans AE: Expression of TrkA, TrkB and TrkC in human neuroblastomas. J Neurooncol 31: 49-55, 1997.
7. Chen S, Caragine T, Cheung NK and Tomlinson S: Surface antigen expression and complement susceptibility of differentiated neuroblastoma clones. Am J Pathol 156: 1085-1091, 2000.
8. Seeger RC, Rayner SA, Banerjee A, Chung H, Laug WE, Neustein HB and Benedict WF: Morphology, growth, chromosomal pattern and fibrinolytic activity of two new human neuroblastoma cell lines. Cancer Res 37: 1364-1371, 1977.
9. Ross RA, Spengler BA and Chang TD: Transdifferentiation of neuroblastoma cells. J Natl Cancer Inst 71: 741-747, 1983.
10. Spengler BA, Lazarova DL, Ross BA and Biedler JL: Cell lineage and differentiation state are primary determinants of MYCN gene expression and malignant potential in human neuroblastoma cells. Oncol Res 9: 467-476, 1997.
11. Ciccarone V, Spengler BA, Meyers MB, Biedler JL and Ross RA: Phenotypic diversification in human neuroblastoma cells: expression of distinct neural crest lineages. Cancer Res 49: 219-225, 1989.
12. Biedler JL, Spengler BA and Ross RA: Transdifferentiation of human neuroblastoma cells results in coordinate loss of neuronal and malignant properties. Prog Clin Biol Res 271: 265-276, 1988.
13. Brodeau GM, Pritchard J, Berthold F, Carlsen NL, Castel V, Castelberry RP, De Bernardi B, Evans AE, Favrot M, Hedborg F, Kaneko M, Kemshead J, Lampert F, Lee RE, Look AT, Pearson AD, Philip T, Roald B, Sawada T, Seegel RC, Tsuchida Y and Voute PA: Revisions of the international criteria for neuroblastoma diagnosis, staging, and response to treatment. J Clin Oncol 11: 1466-1477, 1993.
14. Matsumura T, Iehara T, Sawada T and Tsuchida Y: Prospective study for establishing the optimal therapy of infantile neuroblastoma in Japan. Med Pediatr Oncol 31: 210, 1998.
15. Kaneko M, Nishihara H, Mugishima H, Ohnuma N, Nakada K, Kawa K, Fukuzawa M, Suita S, Sera Y and Tsuchida Y: Stratification of treatment of stage 4 neuroblastoma patients based on N-myc amplification status: study group of Japan for treatment of advanced neuroblastoma. Med Pediatr Oncol 31: 1-7, 1998.
16. Bomken SN, Redfern K, Wood KM, Reid MM and Tweddle DA: Limitations in the ability of NB84 to detect metastatic neuroblastoma cells in bone marrow. J Clin Pathol 59: 927-929, 2006.
17. Thomas JO, Nijjar J, Turley H, Micklem K and Gatter KC: NB84: a new monoclonal antibody for the recognition of neuroblastoma in routinely processed material. J Pathol 163: 69-75, 1991.
18. Janet T, Ludecke G, Otten U and Unsicker K: Heterogeneity of human neuroblastoma cell lines in their proliferative responses to basic FGF, NGF, and EGF: correlation with expression of growth factors and growth factor receptors. J Neurosci Res 40: 707-715, 1995.
19. Nakagawara A: The NGF story and neuroblastoma. Med Pediatr Oncol 31: 113-115, 1998.
20. Sonnenfeld KH and Ishii DH: Nerve growth factor effects and receptors in cultured human neuroblastoma cell lines. J Neurosci Res 8: 375-391, 1982.
21. Chen J, Chattopadhyay B, Venkatakrishnan G and Ross AH: Nerve growth factor-induced differentiation of human neuroblastoma and neuroepithelioma cell lines. Cell Growth Differ 1: 79-85 1990.
22. Chen J, Liu TH and Ross AH: Expression of recombinant NGF receptor in human neuroblastoma cell line without NGF receptor. Basic Med Sci Clin 11: 26-31, 1991.

Silencing Ku80 using small interfering RNA enhanced radiation sensitivity *in vitro* and *in vivo*

YOSHINORI NIMURA[1,6], TETSUYA KAWATA[2], KATSUHIRO UZAWA[3], JUNKO OKAMURA[2], CUIHUA LIU[2], MASAYOSHI SAITO[2], HIDEAKI SHIMADA[1,4], NAOHIKO SEKI[1,5], AKIRA NAKAGAWARA[6], HISAO ITO[2], TAKENORI OCHIAI[1,4] and HIDEKI TANZAWA[1,3]

[1]21st Century Center of Excellence Program, [2]Department of Radiology, [3]Clinical Molecular Biology, [4]Academic Surgery, and [5]Functional Genomics, Chiba University Graduate School of Medicine; [6]Division of Biochemistry, Chiba Cancer Center Research Institute, Chiba, Japan

Received February 5, 2007; Accepted March 21, 2007

Abstract. Ku80 is an important component of DNA double-strand break repair, and Ku80 deficiency leads to extreme sensitivity to ionizing radiation. We studied whether radiation therapy combined with Ku80 silencing by small interfering RNA enhances radiation sensitivity *in vitro* and *in vivo*. Seven human cancer cell lines were transfected with Ku80 siRNA included in hemagglutinating virus of Japan envelope vector. H1299 cells were implanted into male BALB/C nu/nu nude mice treated with Ku80 siRNA and irradiation. The survival rate of cell lines transfected with Ku80 siRNA decreased by 10% to 26% with 2-Gy irradiation compared with untransfected cell lines. The gamma-H2AX phosphorylation-positive rates of Ku80 siRNA combined treatment 0.5 h after irradiation in A549 cells and 6 h in H1299 cells were significantly higher (77.6%, p=0.033 and 76.7%, p=0.026, respectively), compared with the groups not treated with siRNA. H1299 xenograft tumors treated with combined therapy decreased in volume and re-grew slowly compared with radiation alone. Our results indicate that combined therapy consisting of Ku80 siRNA and irradiation contributes to inhibition of tumor growth and may be a novel strategy for cancer treatment.

Correspondence to: Professor Hideki Tanzawa, 21st Century Center of Excellence Program, Chiba University Graduate School of Medicine, 1-8-1 Inohana, Chuo-ku, Chiba 260-8677, Japan
E-mail: tanzawap@faculty.chiba-u.jp

Abbreviations: DSBs, double-strand breaks; NHEJ, non-homologous end-joining; DNA-PKcs, DNA-dependent protease kinase catalytic subunits; siRNA, small interfering RNA; HVJ, hemagglutinating virus of Japan; HVJ-E, HVJ envelope; PBS, phosphate-buffered saline; xrs-5, X-ray-sensitive mutant 5; CHO K1, Chinese hamster ovary

Key words: Ku80, small interfering RNA, HVJ envelope, radiation sensitivity

Introduction

Radiation therapy is a standard treatment for patients with many kinds of cancers. Therapeutic strategies and protocols have been developed and the effectiveness of radiation therapy has greatly improved. However, it is difficult to predict the efficacy and side effects before therapy. Even in patients with the same stage of carcinoma, different responses and resistance to radiation therapy frequently affect the therapy. Radiation therapy with enhanced efficacy using a molecular technique is not yet established. A novel strategy based on a biologic mechanism should optimize the treatment of patients with carcinoma.

DNA double-strand breaks (DSBs) are potentially lethal DNA lesions induced by ionizing radiation (1,2). DSBs can be repaired by homologous recombination or non-homologous end-joining (NHEJ) (1,2). In mammals, NHEJ is especially important for repairing radiation-induced DSBs. Several factors, including Ku70, Ku80, DNA-dependent protease kinase catalytic subunits (DNA-PKcs), artemis, X-ray-complementation group 4, and DNA ligase IV, participate in this pathway (3-5). Ku works in a comparatively early stage. The Ku70/80 complex binds to the DSB ends, recruits DNA-PKcs, and initiates repair (3,6). Ku deficiency leads to extreme sensitivity to radiation (7,8).

Small interfering RNA (siRNA), has been used widely to silence gene expression, and has been evaluated as an attractive tool for use in therapeutics of many cancers (9-14). Some studies have reported that silencing the various repair genes, *ATM*, *ATR*, and *DNA-PKcs* (15,16), *Rad51* (17), *NBS1* (18,19), and *Mre11* (20), increased radiation sensitivity. However, the efficacy of Ku80 silencing for radiation sensitivity has not yet been evaluated.

siRNA technology is a powerful method of gene down-regulation; however, *in vivo*, it has been difficult to achieve high efficacy using the siRNA delivery system. The hemagglutinating virus of Japan (HVJ; Sendai virus) envelope vector is a new reagent for the transfection of DNA, protein, and oligonucleotides (21-26). The HVJ envelope (HVJ-E) vector was constructed with inactivated particles and therefore has no viral activity. Using the HVJ-E system, the efficiency of

gene transfer into various cell lines is greatly enhanced, even when injected into organs directly in *in vivo* experiments (21-23).

We hypothesized that radiation therapy combined with Ku80 silencing might enhance radiation sensitivity, because of the reduced reparative ability of DSBs. In the current study, the expression of Ku80 was alternately inhibited using siRNA included in HVJ-E, and we studied *in vitro* and *in vivo* whether radiation sensitivity could be enhanced regardless of the type and radiation survival rate of the cancer cell lines.

Materials and methods

Cell lines and treatment. A549 and H1299 cells, which are lung carcinomas, were obtained from the American Type Culture Collection (Rockville, MD). A549 cells express normal p53, and H1299 cells are null for the *p53* gene. TE13 (esophageal carcinoma), PANC-1 (pancreas carcinoma), MIAPaCa-2 (pancreas carcinoma), DU-145 (prostate carcinoma), and ME-180 (cervical carcinoma) cells were obtained from the Cell Resource Center for Biomedical Research Institute of Development, Aging and Cancer Tohoku University (Miyagi, Japan). All cells were maintained as a monolayer in Dulbecco's modified Eagle's medium (Sigma, St. Louis, MO), supplemented with 10% fetal bovine serum, and grown at 37°C in a humidified atmosphere of 5% carbon dioxide. Exponentially grown cells were used for all experiments.

Clonogenic assay. To evaluate radiation sensitivity, surviving fractions were measured using a standard colony-formation assay (27). Briefly, the cells were counted and the appropriate number seeded into 60-mm dishes in triplicate for each dose. Six hours later, when all cells had attached but not yet divided, the cells were irradiated with doses ranging from 0 to 6-Gy using an MBR-1520R-3 (Hitachi, Tokyo, Japan) generator operated under 150 kVp and 20 mA with a 1-mm aluminum filter. The dose rate was about 2-Gy/minute. Colonies obtained after 10 to 14 days were stained with crystal violet and contained >50 cells.

siRNA transfection. The siRNA used for Ku80 gene silencing was designed by Qiagen (Valencia, CA). The target sequence was AAG CGA GTA ACC AGC TCA TAA, and the siRNA sense sequence was r(GCG AGU AAC CAG CUC AUA A)dTdT.

Transfection of Ku80 siRNA was conducted with HVJ-E according to the manufacturer's recommendations (Ishihara Sangyo Kaisha, Ltd., Osaka, Japan). Briefly, cells were seeded into 6-well plates for 24 h before siRNA transfection. One microgram of siRNA was prepared to make complexes with HVJ-E according to the manufacturer's instructions (Ishihara Sangyo Kaisha, Ltd.). Several cell lines were transfected with Ku80 siRNA included in HVJ-E in medium supplemented with 10% fetal bovine serum. Forty hours after transfection, the cells were trypsinized and some were irradiated for clonogenic assay. The rest of the cells were lysed to extract protein for Western blotting.

Western blot analysis. Cells were lysed in lysis buffer [50 mM Tris-HCl (pH 8.0), 450 mM NaCl, 1% Triton X-100, 1 mM EDTA (pH 8.0), and 0.6 mM PMSF] containing a protein inhibitor cocktail (4-benzenesulfonyl, fluoride, pepstatin A, E-64, bestatin, leupeptin, and aprotinin) (Sigma). Protein concentrations of lysates were determined using a protein assay kit (Bio-Rad, Hercules, CA). Forty micrograms of protein was loaded and electrophoresed on 10% sodium dodecyl sulfate polyacrylamide gels. After blotting the nitrocellulose membranes, the protein was probed with primary mouse monoclonal Ku70, Ku80 (Santa Cruz Biotechnology, Inc., Santa Cruz, CA), and ß-actin (Sigma) antibodies then with secondary horseradish peroxidase-conjugated goat anti-mouse IgG antibody (Santa Cruz Biotechnology, Inc.). The immunoreactive bands were visualized using enhanced chemiluminescence on X-ray film (ECL Western Blotting Detection Reagent, GE Healthcare Bio-Sciences Corp., Piscataway, NJ).

Immunofluorescent staining for gamma-H2AX. Cells were seeded onto chamber slides (Nalge Nunc International, Naperville, IL) and transfected with the HVJ-E vector containing Ku80 siRNA for 40 h according to the manufacturer's instructions (Ishihara Sangyo Kaisha, Ltd.). After transfection, the cells were irradiated with 2-Gy or treated immediately without irradiation. Irradiated cells were treated using the following procedure after 30 min or 6 h. The cells were fixed with 1% paraformaldehyde solution in phosphate-buffered saline (PBS) for 30 min at room temperature, soaked in -20°C 99% methanol for 5 min, and incubated in 3% bovine serum albumin with 0.2% Tween-20 in PBS for 1 h at 37°C. The cells were probed in primary mouse monoclonal anti-phospho-H2A.X (ser139) antibody (Upstate Biotechnology, Lake Placid, NY) at a dilution of 1:300 for 1.5 h at 37°C and then in secondary Cy2-goat anti-rabbit IgG antibody at a dilution of 1:400 for 1 h at room temperature.

Fluorescence images were captured by Axioskop2 plus confocal microscopy equipped with a CCD camera and quantitated using AxioVisio Release 4.3 software (Carl Zeiss, Oberkochen, Germany). Significant colocalization of nuclear foci was determined by visualization of green spots on a DAPI background.

Gamma-H2AX foci were determined in five fields and at least 50 cells of each experiment. The cells were classified as positive when more than 10 foci were counted in the nucleus.

In vivo xenograft model. In vivo studies were carried out in accordance with the Guidelines for Animal Experimentation of Chiba University. Four-week-old male BALB/C nu/nu nude mice were obtained from Charles River Japan Inc. (Yokohama, Japan). To generate tumor xenografts, 5.0×10^6 viable H1299 cells were subcutaneously injected into the right hind legs. Tumors were measured in two dimensions with calipers and the volume was estimated using the following calculation: (major axis) x (minor axis) x (minor axis) x 1/2.

We generated two protocols, one for one fraction and the other for five fractions. For one fraction, when the tumors reached 150-200 mm^3 (day 0), the mice were randomly divided into three groups: control (no radiation; n=11), radiation alone (4-Gy in one fraction on day 1; n=6), and Ku80 siRNA treatment with radiation (siRNA injection on day 0 and 4-Gy in one fraction on day 1; n=6). For five

fractions, when the tumors reached 750-1000 mm^3 (day 0), the mice were randomly divided into three groups: control (no radiation; n=10), radiation alone (4-Gy in one fraction on days 1, 2, 3, 4, and 5; n=7), and Ku80 siRNA treatment with radiation (siRNA injection on days 2 and 4, and 4-Gy in one fraction on days 1, 2, 3, 4, and 5; n=8).

Gene delivery. H1299 xenograft tumors in the hind legs of nude mice were treated with Ku80 siRNA included in HVJ-E. The HVJ-E complex included Ku80 siRNA prepared as previously described. Ku80 siRNA was injected directly into the tumors. Each injection was diluted in a total volume of 50 μl of 0.9% sodium chloride solution and administered in one pass using a 27-gauge needle.

Statistical analysis. Statistical analysis was performed using SigmaStat 3.1 (Point Richmond, CA). For a single comparison, the level of statistical significance was confirmed using Student's t test. $p<0.05$ were considered statistically significant.

Results

Down-regulation of Ku80 protein expression by siRNA in A549 and H1299 cells. To determine whether Ku80 silencing contributes to radiation sensitivity, two siRNAs were designed and screened for the ability to down-regulate target protein expression. To determine the best protocol for silencing Ku80 protein expression, the cells were transfected with siRNA/HVJ-E complexes at various times, and protein extracts were obtained from 6 to 96 h after transfection. Western blot analyses showed that siRNA/HVJ-E complexes minimized Ku80 expression 40 h after transfection compared with untransfected cells (data not shown). We used 40 h of treatment with siRNA for the experiments.

Western blot analysis of Ku80 protein expression in A549 and H1299 cells was performed 40 h after transfection with Ku80 siRNA (Fig. 1A). Ku80 protein expression was suppressed, indicating successful gene silencing by siRNA. In cells transfected with Ku80 siRNA, Ku80 protein decreased compared with the transfected HVJ-E or the untransfected cells. Interestingly, although the cells were transfected with Ku80 siRNA, Ku70 protein expression also was suppressed and correlated with Ku80 expression level in both cell lines. The A549 cells are wild-type cells of the *p53* gene and the H1299 cells are the null type. The efficiency of the suppression did not depend on the *p53* gene status.

Cellular sensitivity after treatment with Ku80 siRNA. The A549 and H1299 cells exhibited a typical clonogenic survival curve with a shoulder signifying cellular repair capacity. Doses of 2, 4, and 6-Gy of irradiation alone killed about 31, 60, and 84% of the A549 cells, and 21, 53, and 76% of the H1299 cells, respectively (Fig. 1B). Furthermore, the survival rates of cells transfected with HVJ-E alone were close to the rate for the original cells. However, Ku80 siRNA enhanced cell killing in 57, 86, and 96% of the A549 cells and 35, 71, and 90% of the H1299 cells, respectively. siRNA inhibition of Ku80 protein confirmed enhanced radiation sensitivity in siRNA-transfected cells compared with the transfected

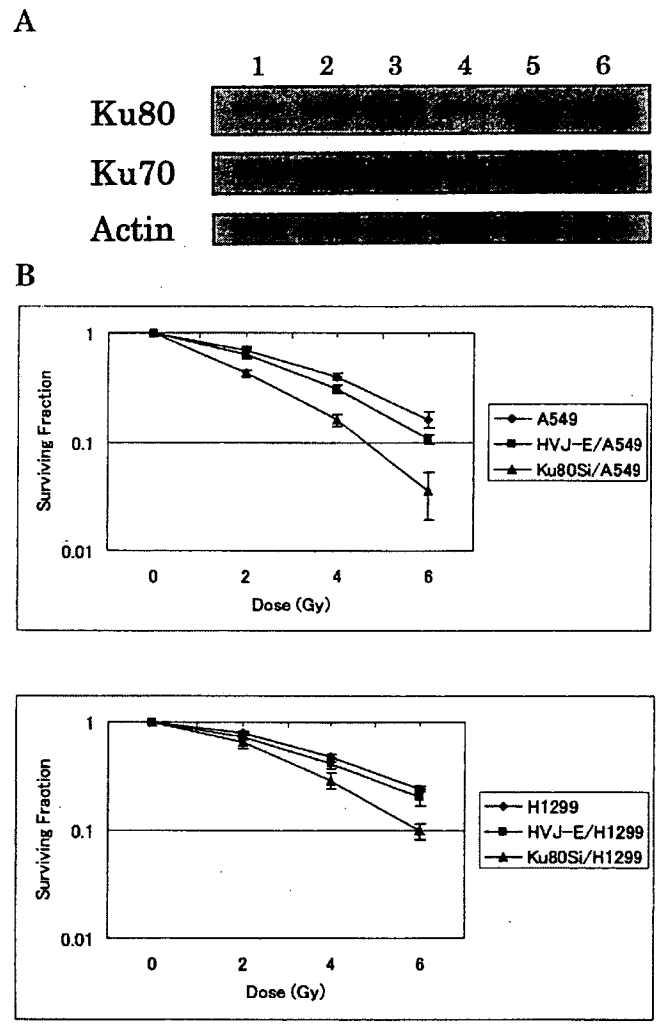

Figure 1. Down-regulation of Ku80 protein and radiation sensitivity in A549 and H1299 cells. Western blotting: after treatment with HVJ-E including Ku80 siRNA for 40 h, the protein expression of Ku80 is suppressed compared with the cell lines without siRNA or those treated with only HVJ-E. Actin serves as a loading control. Lane 1, Ku80si/A549; lane 2, HVJ-E/A549; lane 3, A549; lane 4, Ku80si/H1299; lane 5, HVJ-E/H1299; and lane 6, H1299 (A). Clonogenic assay: in the cell line treated with Ku80 siRNA, the surviving fraction of the A549 cells treated with 2-Gy irradiation is reduced by 26%, and the surviving fraction of the H1299 cells is reduced by 14% compared with the untreated cell line. Radiation sensitivity is enhanced by treatment with Ku80 siRNA. All experiments were performed in triplicate. Data are presented as the mean ± SE (B).

HVJ-E or the untransfected cells. We focused on the results of 2-Gy irradiation, which is the usual dose for a single fraction in the clinic. The increased radiation sensitivity at 2-Gy irradiation corresponded to 26 and 14% for Ku80 silencing in the A549 and H1299 cells, respectively.

Radiation sensitivity enhancement by Ku80 siRNA in several human cancer cell lines. After controlling and suppressing Ku80 in tumor cells alternately using siRNA, it was important to verify if radiation sensitivity can be enhanced regardless of the modality and radiation survival rate of a tumor. Another five cancer cell lines, TE13, PCNA-1, MIAPaCa-2, DU-145, and ME-180, were selected for the Ku80 siRNA experiments, because radiation therapy is usually effective for these cancers. Western blot analyses of Ku80 protein expression in all cell

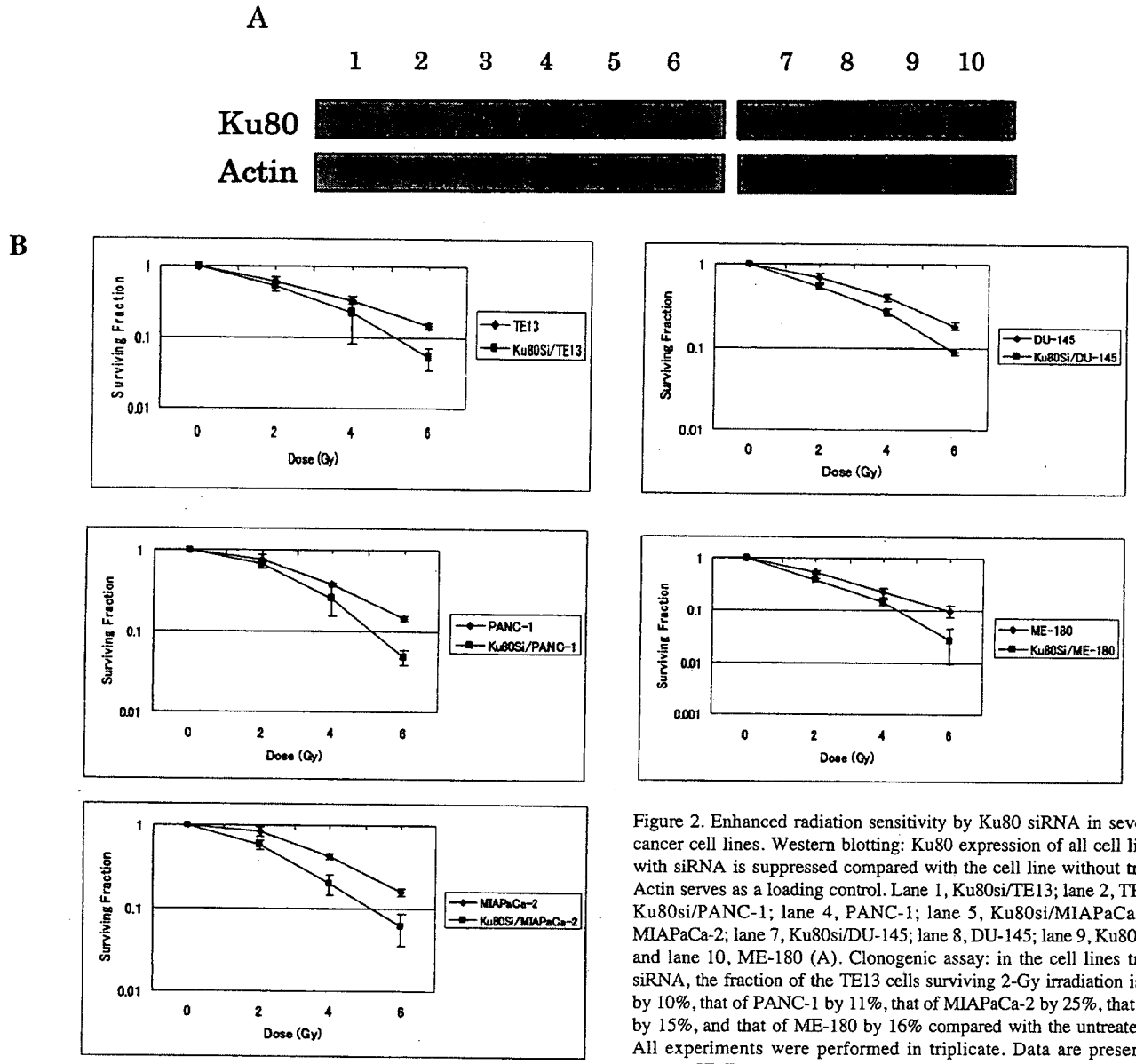

Figure 2. Enhanced radiation sensitivity by Ku80 siRNA in several human cancer cell lines. Western blotting: Ku80 expression of all cell lines treated with siRNA is suppressed compared with the cell line without transfection. Actin serves as a loading control. Lane 1, Ku80si/TE13; lane 2, TE13; lane 3, Ku80si/PANC-1; lane 4, PANC-1; lane 5, Ku80si/MIAPaCa-2; lane 6, MIAPaCa-2; lane 7, Ku80si/DU-145; lane 8, DU-145; lane 9, Ku80si/ME-180; and lane 10, ME-180 (A). Clonogenic assay: in the cell lines treated with siRNA, the fraction of the TE13 cells surviving 2-Gy irradiation is decreased by 10%, that of PANC-1 by 11%, that of MIAPaCa-2 by 25%, that of DU-145 by 15%, and that of ME-180 by 16% compared with the untreated cell line. All experiments were performed in triplicate. Data are presented as the mean ± SE (B).

lines were performed as described previously. After transfection of Ku80 siRNA, Ku80 protein expression was suppressed compared with the untransfected cells (Fig. 2A).

In the cell lines treated with siRNA, surviving fractions of TE13 treated with 2-Gy irradiation decreased by 10% that of PANC-1 by 11%, that of MIAPaCa-2 by 25%, that of DU-145 by 15%, and that of ME-180 by 16% compared with untreated cell lines (Fig. 2B). We observed enhanced radiation sensitivity regardless of the cancer type.

Reduced reparative ability of DSBs resulting from combined radiation and siRNA treatment. Ku80 siRNA apparently enhanced radiation sensitivity in several human cancer cell lines. According to the biologic mechanism, we hypothesized that radiation therapy combined with Ku80 silencing would reduce the DSBs reparative ability. Thus, immunofluorescence detection of gamma-H2AX nuclear foci was performed to detect DSBs.

Gamma-H2AX foci were detected after 2-Gy irradiation in the A549 and H1299 cells. Gamma-H2AX foci stained green; all cells counterstained blue with DAPI for nuclear DNA (data not shown). When >10 gamma-H2AX foci were seen in the cell, it was determined as positive. In both cell lines, positive rates of gamma-H2AX foci immediately increased and decreased over time. The two positive rates with siRNA, at 0.5 h after irradiation in A549 cells and at 6 h in H1299 cells, were significantly higher by 77.6% (95% CI, 70-85; p=0.033) and 76.7% (95% CI, 68-86; p=0.026) compared with no siRNA treatment, 64.1 and 57.5%, respectively (Fig. 3). This suggested that the ability of the DSB repair decreased after radiation and siRNA treatment compared with radiation alone.

Suppression of tumor growth by Ku80 siRNA in H1299 xenograft models. To examine further effects of Ku80 siRNA, we conducted *in vivo* experiments with H1299 xenograft tumors. We used the *in vivo* radiation dose of 4-Gy to simplify ascertaining the effect after treatment.

Before testing the two protocols, we first investigated the post-irradiation effects to estimate the efficiency of Ku80